



AFRL-RX-TY-TR-2012-0051

**ADVANCED INTEGRATED POWER SYSTEMS
(AIPS)**

Keith A. Kozlowski, Christian D. Rasmussen
Applied Research Associates, Inc.
421 Oak Drive
Panama City, FL 32401

Reza Salavani, Lucas M. Martinez, Marcus D. Smith
Airbase Technologies Division
Air Force Research Laboratory
139 Barnes Drive, Suite 2
Tyndall Air Force Base, FL 32403-5323

Contract No. FA4819-09-C-0031

October 2012

DISTRIBUTION A: Approved for public release; distribution unlimited.
88ABW-2012-5348, 10 October 2012.

**AIR FORCE RESEARCH LABORATORY
MATERIALS AND MANUFACTURING DIRECTORATE**

DISCLAIMER

Reference herein to any specific commercial product, process, or service by trade name, trademark, manufacturer, or otherwise does not constitute or imply its endorsement, recommendation, or approval by the United States Air Force. The views and opinions of authors expressed herein do not necessarily state or reflect those of the United States Air Force.

This report was prepared as an account of work sponsored by the United States Air Force. Neither the United States Air Force, nor any of its employees, makes any warranty, expressed or implied, or assumes any legal liability or responsibility for the accuracy, completeness, or usefulness of any information, apparatus, product, or process disclosed, or represents that its use would not infringe privately owned rights.

NOTICE AND SIGNATURE PAGE

Using Government drawings, specifications, or other data included in this document for any purpose other than Government procurement does not in any way obligate the U.S. Government. The fact that the Government formulated or supplied the drawings, specifications, or other data does not license the holder or any other person or corporation; or convey any rights or permission to manufacture, use, or sell any patented invention that may relate to them.

This report was cleared for public release by the 88th Air Base Wing Public Affairs Office at Wright Patterson Air Force Base, Ohio available to the general public, including foreign nationals. Copies may be obtained from the Defense Technical Information Center (DTIC) (<http://www.dtic.mil>).

AFRL-RX-TY-TR-2012-0051 HAS BEEN REVIEWED AND IS APPROVED FOR PUBLICATION IN ACCORDANCE WITH ASSIGNED DISTRIBUTION STATEMENT.

SALAVANI.REZA. Digitally signed by SALAVANI.REZA.1230156944
DN: c=US, o=U S Government, ou=DoD, ou=PKI,
ou=USAF, cn=SALAVANI.REZA.1230156944
Date: 2012.09.20 16 03:19 -0500
1230156944

REZA SALAVANI
Work Unit Manager & Program Manager

RHODES.ALBERT Digitally signed by
RHODES.ALBERT.N.III.1175488622
DN: c=US, o=U S Government, ou=DoD, ou=PKI,
ou=USAF, cn=RHODES.ALBERT.N.III.1175488622
Date: 2012.10.02 15 22:05 -0500
.N.III.1175488622

ALBERT N. RHODES, PhD
Chief, Airbase Technologies Division

This report is published in the interest of scientific and technical information exchange, and its publication does not constitute the Government's approval or disapproval of its ideas or findings.

REPORT DOCUMENTATION PAGE

*Form Approved
OMB No. 0704-0188*

The public reporting burden for this collection of information is estimated to average 1 hour per response, including the time for reviewing instructions, searching existing data sources, gathering and maintaining the data needed, and completing and reviewing the collection of information. Send comments regarding this burden estimate or any other aspect of this collection of information, including suggestions for reducing the burden, to Department of Defense, Washington Headquarters Services, Directorate for Information Operations and Reports (0704-0188), 1215 Jefferson Davis Highway, Suite 1204, Arlington, VA 22202-4302. Respondents should be aware that notwithstanding any other provision of law, no person shall be subject to any penalty for failing to comply with a collection of information if it does not display a currently valid OMB control number.

PLEASE DO NOT RETURN YOUR FORM TO THE ABOVE ADDRESS.

1. REPORT DATE (DD-MM-YYYY) 08-OCT-2012	2. REPORT TYPE Final Technical Report	3. DATES COVERED (From - To) 01-OCT-2007 -- 30-JUN-2012
---	---	---

4. TITLE AND SUBTITLE Advanced Integrated Power Systems (AIPS)	5a. CONTRACT NUMBER FA4819-09-C-0031
	5b. GRANT NUMBER
	5c. PROGRAM ELEMENT NUMBER 0603112F

6. AUTHOR(S) *Kozlowski, Keith A.; *Rasmussen, Christian D.; ^Salavani, Reza; ^Martinez, Lucas M.; ^Smith, Marcus D.	5d. PROJECT NUMBER 4915
	5e. TASK NUMBER D0
	5f. WORK UNIT NUMBER Q110D8B3

7. PERFORMING ORGANIZATION NAME(S) AND ADDRESS(ES) *Applied Research Associates, Inc. 421 Oak Drive Panama City, FL 32401	8. PERFORMING ORGANIZATION REPORT NUMBER
---	---

9. SPONSORING/MONITORING AGENCY NAME(S) AND ADDRESS(ES) ^Air Force Research Laboratory Materials and Manufacturing Directorate Airbase Technologies Division 139 Barnes Drive, Suite 2 Tyndall Air Force Base, FL 32403-5323	10. SPONSOR/MONITOR'S ACRONYM(S) AFRL/RXQES
	11. SPONSOR/MONITOR'S REPORT NUMBER(S) AFRL-RX-TY-TR-2012-0051

12. DISTRIBUTION/AVAILABILITY STATEMENT
Distribution A: Approved for public release; distribution unlimited.

13. SUPPLEMENTARY NOTES
Ref Public Affairs Case # 88ABW-2012-5348, 10 October 2012. Document contains color images.

14. ABSTRACT
The objective of this effort was to determine the ability to save fuel used for generating electricity in an austere location for a military deployment application. The contractor performed testing of four different systems with two different loading scenarios. The loading scenarios were based off a repeatable block program to allow direct comparison of different systems. The results showed that the system with both energy storage and solar energy saved approximately 43% of the fuel consumed by the baseline system, while just adding energy storage showed 23% savings. The test also revealed that almost no savings were achieved by adding solar power without energy storage. Comparing the baseline system at the two loads indicated that a 32% reduction in energy demand resulted in only 12% reduction in fuel consumption by generators.

15. SUBJECT TERMS
power generation, power switching, load sharing, voltage control

16. SECURITY CLASSIFICATION OF:			17. LIMITATION OF ABSTRACT UU	18. NUMBER OF PAGES 62	19a. NAME OF RESPONSIBLE PERSON Reza Salavani
a. REPORT U	b. ABSTRACT U	c. THIS PAGE U			19b. TELEPHONE NUMBER (Include area code)

Reset

TABLE OF CONTENTS

LIST OF FIGURES	ii
LIST OF TABLES	iii
1. SUMMARY	1
2. INTRODUCTION	2
2.1. Background	2
2.2. Literature Review.....	4
2.2.1. Other Military Experiments	4
2.2.2. Published Literature Review.....	4
3. METHODS, ASSUMPTIONS, AND PROCEDURES.....	8
3.1. Test Site Location	8
3.2. Test Equipment	8
3.2.1. Component Panel Board Equipment.....	8
3.2.2. Data Acquisition Enclosure Equipment.....	11
3.2.3. RETC Outdoor Equipment	13
3.2.4. System Diagram.....	17
3.3. Test Procedures.....	18
3.3.1. Test Protocols.....	18
4. RESULTS AND DISCUSSION	33
4.1. Fuel Consumption.....	33
4.2. Detailed Power Data	33
4.2.1. Data Calibration	33
4.2.2. System Data	34
5. CONCLUSIONS.....	42
6. REFERENCES	43
Appendix A: Equipment Specifications.....	45
Appendix B: AIPS Electrical Schematic Diagrams.....	53
LIST OF SYMBOLS, ABBREVIATIONS, AND ACRONYMS	58

LIST OF FIGURES

	Page
Figure 1. Deloitte Analysis of Casualties vs. Fuel Consumption	2
Figure 2. Schematic of Current BEAR Base Power Plant	3
Figure 3. Renewable Energy Tent City, Tyndall AFB	8
Figure 4. Component Panel Board (Front)	9
Figure 5. Component Panel Board (Back)	9
Figure 6. Xantrex XW Hybrid Inverter/Charger	10
Figure 7. Xantrex XW Solar Charge Controller	10
Figure 8. Deka/MK Unigy II Energy Storage System	11
Figure 9. Data Acquisition Enclosure	11
Figure 10. National Instruments cRIO Hardware	12
Figure 11. National Instruments Panel PC	12
Figure 12. LabVIEW VI	13
Figure 13. MEP-805A 30 kW Generator	14
Figure 14. Secondary Distribution Center (SDC)	14
Figure 15. Power Distribution Panel (PDP)	14
Figure 16. PV Array System Top	15
Figure 17. PV Array System Side	15
Figure 18. PV Array System Wiring	15
Figure 19. Utilis Shelter with Konarka Panel Solar Fly	16
Figure 20. Konarka Panel Electrical Grouping	16
Figure 21. System Diagram	17
Figure 22. Electrical Connection of System	17
Figure 23. System 1 Test Configuration	20
Figure 24. AIPS Fuel Log Data Example	21
Figure 25. System 4 Test Configuration	23
Figure 26. System 2 Test Configuration	25
Figure 27. System 2 and 3 Load Sequence Example for a 24-hr Period	25
Figure 28. 10 percent D.O.D Time Limits for Energy Storage Power Supply	27
Figure 29. System 3 Test Configuration	29
Figure 30. System 3 Energy Storage Charge State 1	31
Figure 31. System 3 Energy Storage Charge State 2	31
Figure 32. Calibration Curves	34
Figure 33. System 1/Load Scenario 1	35
Figure 34. System 2/Load Scenario 1	35
Figure 35. System 3/Load Scenario 1	36
Figure 36. System 3/Load Scenario 1, Available vs. Used Solar Power	36
Figure 37. System 4/Load Scenario 1	37
Figure 38. System 4/Load Scenario 1, Available Solar Power	38
Figure 39. System 1/Load Scenario 2	38
Figure 40. System 2/Load Scenario 2	39
Figure 41. System 3/Load Scenario 2	39
Figure 42. System 3/Load Scenario 2, Available vs. Used Solar Power	40
Figure 43. System 4/Load Scenario 2	40
Figure 44. System 4/Load Scenario 2 Available Solar Power	41

LIST OF TABLES

	Page
Table 1. Component Panel Board Equipment List	9
Table 2. Data Acquisition Enclosure Equipment List	11
Table 3. Tent City Outdoor Equipment	13
Table 4. Load Block Schedule	19
Table 5. High Load—Baseline System Test Matrix	19
Table 7. High Load - System with Solar Panels Test Matrix	22
Table 8. Low Load - System with Solar Panels Test Matrix	22
Table 9. High Load - System with Energy Storage Test Matrix	23
Table 10. Low Load - System with Energy Storage Test Matrix	24
Table 11. High Load - Current System with Solar and Energy Storage Test Matrix	28
Table 12. Low Load - Current System with Solar and Energy Storage Test Matrix.....	29
Table 13. Fuel Consumption Comparison	33

1. SUMMARY

Applied Research Associates, in support of the Air Force Research Laboratory (AFRL), performed an experiment to determine the ability to save fuel used to generate electricity in an austere location consistent with a military deployment. The test program evaluated four different systems with two different loading scenarios. The loading scenarios were based off a repeatable block program to allow direct comparison of different systems.

The test systems comprised a baseline system, similar to current Air Force Basic Expeditionary Airfield Resource (BEAR) Base power production methodologies, a system with added energy storage which allowed the generator to cycle on and off, a system with added energy storage plus significant amounts of solar energy, and a system with the same solar energy capability, but without energy storage.

The results show that the system with both energy storage and solar energy saved approximately 43 percent of the fuel consumed by the baseline system, while just adding energy storage showed 23 percent savings. The test also revealed that almost no savings were achieved by adding solar power without energy storage.

Comparing the baseline system at the two loads shows that a 32 percent reduction in energy demand results in only a 12 percent reduction in generator fuel consumed.

2. INTRODUCTION

2.1. Background

The supply of fuel to deployed military or humanitarian missions can represent a significant burden. In the current Air Force BEAR Base standard, an 1100 man deployment consumes 5280 gal of fuel per day. Assuming \$15/gal fully burdened cost, this equates to roughly \$30 million per year per 1100 man deployment just for generator fuel. Further, it is estimated that 70 percent of the fuel used in theater is consumed in direct support of convoys to the front lines, and these convoys are 70 percent by weight fuel (Shaffer March 2009). This equates to roughly half of the fuel in theater being used to deliver fuel. Therefore, a 1-gal reduction in generator fuel consumption or delivery eliminates an additional gallon required to transport and defend the delivery.

In terms of human costs, it is estimated that a significant percentage of our casualties are as a result of ensuring the steady supply of fuel to our in-country bases. Analysis by Deloitte (2009) shows a direct correlation between in theater fuel consumption and casualty rate.

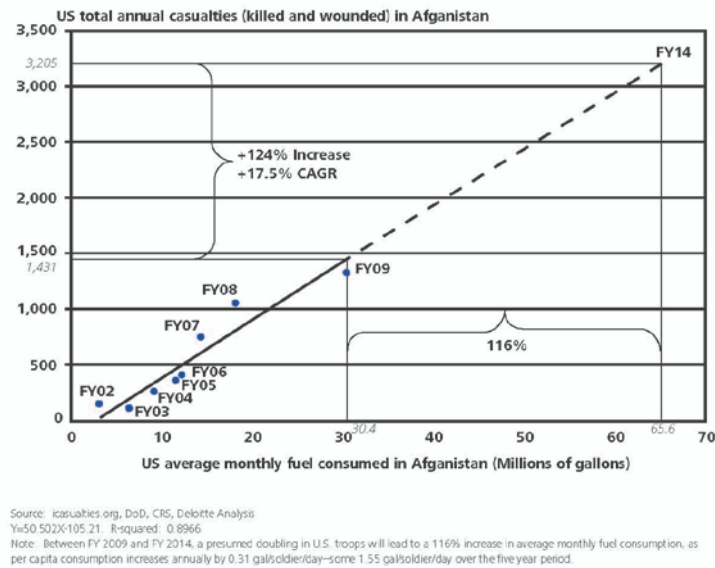


Figure 1. Deloitte Analysis of Casualties vs. Fuel Consumption
Source: (Deloitte 2009, 18)

In his comments at the USMC Expeditionary Power and Energy Symposium, General Conway indicated that the Marine Corps are averaging 22 gal of fuel per day, per person (Conway February 2010). He also indicated that at Camp Leatherneck, the generators were running at around 30 percent capacity, with 15 MW of capacity in production, and 5 MW required.

Because of the high cost, both in blood and treasure, the Air Force is looking for ways to reduce the burden of fuel and to minimize the logistical tail required to support forces in austere locations. To this end, the Air Force's energy reduction framework, as documented in the Air

Force Energy Plan 2010, is built on three pillars: Reduce Consumption, Increase Supply and Culture Change (U.S. Air Force 2010). The Plan also makes a specific end state goal that forward bases must be capable to operate using renewable energy.

The current planning method for producing power in a deployed BEAR Base is based on using four mobile electric power (MEP) 12 generators (750 kW each) as the core power plants, with smaller MEPs also used for spot power generation and backup of critical systems. A single MEP 12 consumes 55 gal/hr of JP8 which equates to 5280 gal/day for an 1100 man encampment. Three phase high voltage (4160 V) power from the generators is connected to a switching station known as a primary distribution panel (PDP), sometimes referred to as a primary distribution center (PDC). The PDP/PDC routes high voltage (4160 V) power out to multiple secondary distribution centers (SDC), which in turn feed the power to the point of need. Figure 2 illustrates the current layout for a deployable base power grid.

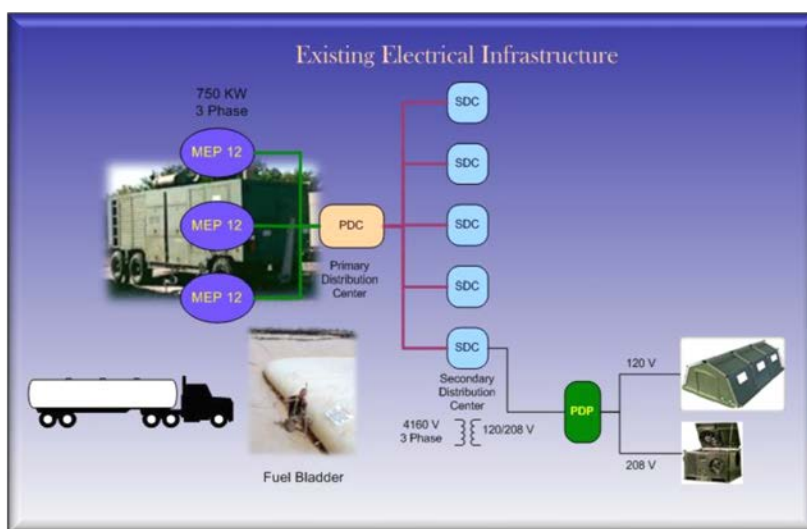


Figure 2. Schematic of Current BEAR Base Power Plant

The current control scheme has inadequate control over power production, loads and distribution systems, and is characterized by a lack of information to provide power related decision making. This lack of information and control leads operational decision makers to adopt a strategy of over-production of electrical capacity, with corresponding over consumption of fuel. This type of control scheme also does not lend itself to distributed power generation, which is concomitant with significant integration of renewable energy.

If we estimate an actual, in-use overproduction of 100 percent (producing twice the needed energy), the model 1100 man camp then consumes 10560 gal/day. While it may seem excessive to assume this magnitude of overproduction, General Conway's comments would lead to estimating that overproduction is more on the order of 200 percent. This larger figure is consistent with anecdotal evidence the authors have gathered from various power managers returning from deployments.

Because of these issues, AFRL developed the Advanced Integrated Power Systems (AIPS) program to investigate ways to provide significant reduction in fuel used for our deployed forces through proper management of generator loads and power production and integration of renewable energy streams in a deployed BEAR Base.

In order to more accurately determine the value of proposed changes in control schemes or hardware, the authors developed a repeatable block schedule approach. The block schedule developed attempts to replicate actual BEAR Base power consumption on a small, repeatable scale by lumping together loads into repeatable blocks of various durations. Our testing schedule is based off of an assumption that in practice, most deployed military power plants are run at or near full capacity at all times without regard to actual loads. The authors have interviewed a number of sources and feel confident that this assumption is valid across many theaters of operation in many different size deployed bases, across all branches of service. The two different load blocks represent a 100 percent overproduction (30 kW generator compared to a max load of 15 kW) and a 200 percent overproduction (30 kW generator compared to a max load of 10 kW).

2.2. Literature Review

2.2.1. Other Military Experiments

Recent (unpublished) studies performed by the Communications-Electronics Research, Development, and Engineering Center (CERDEC), Army Power Division show a 36 percent reduction in fuel consumption by implementing a smart generator control scheme, and estimate up to 50 percent reduction with added energy storage capability. This Army study was performed using spot generation, where there are a large number of small generators, with no central power distribution system. This is dissimilar to the Air Force BEAR Base standard which includes a managed power distribution system (Figure 2).

Other similar experiments are currently ongoing, but results were not available for inclusion in this report.

2.2.2. Published Literature Review

Kariniotakis et al. (2005) studied the interconnection of modular generation and storage technologies for small distribution systems. In this study, they examined various solutions for modeling dynamic loads and sources. For each system, they set up relational equations and system representation models from which dynamic analysis was possible. Their simulation and analysis models were done in Matlab and Simulink. Each type of power generation source could be modeled as a series of admittance equations. The individual power phases (sources and loads) were separated and handled with a relational phase equation.

Oyarzabal et al. (2005) used the Java Development Framework (JADE) to automate their intelligent power system agents. Their system design allowed cooperation between independent agents using goal directed behavior on the mini grid. This system uses a micro grid central controller, pulling agent (data acquisition), database agent, control agent (secondary regulation), shifting agent (shift able loads), curtailment agent, etc. These agents each perform valuable functions in the governance and control of dynamic sources and loads. This system utilizes a messenger transport protocol (MTP) in relation to hypertext transfer protocol (HTTP) for communication between the agents.

Marwali et al. (2004) discusses the control strategy for the parallel operation of distributed generation systems in a standalone alternating current (AC) power supply. The authors achieve control by combining the droop and average power control methods to overcome sensitivity about voltage and current measurement errors. The authors discuss the effectiveness of the presented method from both experimental and simulation results.

Degner et al. (2005) examine the grid impact issues for two case studies involving increased renewable energy source integration on a remote island. The authors examined an island grid which was autonomous, fed primarily by diesel generators. This scenario somewhat mimics a deployed base's electric infrastructure. In this study, the authors examine grid issues of voltage profile, active and reactive power flows, thermal loading on circuit elements, transient stability, dynamic stability, voltage stability, reactive power control, and frequency control.

Casadei et al. (2005) used several different energy storage devices as part of a grid conditioning system. These devices were super-capacitor banks, flywheels, superconducting magnetic energy storage, and advanced batteries (such as Li-ion). Their test system combined the activities of inversion and rectification with energy storage for reactive power compensation, current harmonic reduction, smoothing pulsating loads, etc. This study gives a fairly accurate model for each of these storage devices.

Takeru et al. (2009) developed a 10 kW inverter to examine the performance with high power photovoltaic (PV) modules. The authors indicated that to efficiently use PV power the efficiency of the interactive inverter required improvement. To solve this problem, the authors developed an interactive transformer-less inverter to eliminate the iron and copper losses in the transformer.

Meliopoulos et al. (2002) reported on the need for analysis and design tools for distributed energy sources. In this report, the authors discuss several issues associated with connecting to a distribution system that may operate in parallel or autonomously. They assert the need for three phase analysis and explicit modeling of grounding and bonding of the system as key components in distributed energy design.

Jayawarna et al. (2005) focuses on the electrical safety concerns associated with the integration of distributed generation system in a microgrid environment. Fault current distribution during islanded and grid-connected operation was the primary issue investigated. Their paper describes an earthing or grounding system design for integration into a microgrid. Their design would rely on over current sensing technologies that are designed for an inverter based grid environment.

O’Gorman (2005) discusses the value of voltage control for distributed generation systems. Lower power factors result in less efficient energy transfer. This paper suggests that each distributed generation system assist in maintaining the voltage quality at its own terminals by adjusting the active and reactive power components. This will result in a variable power factor seen by the grid system to which the generation system is attached as well as allowing the generator to contribute power to the grid. The grid tie controller must have an adaptive algorithm to allow power to flow in both directions as well as adjustments for phase and reduction of

harmonic components. The interaction between controllers is vital as well as sensors to measure phase lag and maximum power point tracking.

Leung (1997) discusses new fault current mitigation techniques in a power grid using a superconducting fault-current limiter. The superconductors would change from a near zero impedance during normal operation to a very high impedance during a fault. This device relies on the use of high temperature superconductors (HTS) in conjunction with fast power electronics that can react to a fault in less than 1 cycle.

Michigami et al. (2002) discuss how the creation of a dynamic load model based on a series of field measurement experiments. The dynamic model included aspects of the fluctuation load component and the fluctuation frequency as well as the time domain load variance seen on the grid. This algorithm calculates the ratio of the fluctuation load to the total power demand. The actual model was constructed by multiplying white noise (normal distribution) with the measured base and fast fringe loads and the resultant values are summed. The model-generated results were compared to actual data to verify the validity of the model. The model can now be used with microgrid models to simulate control and response strategies.

Shinji et al. (2008) discusses methods of reducing power fluctuations in an islanded microgrid. Their primary approach is the introduction of gas turbines (future design includes large NaS grid batteries since the control over fluctuations requires an inefficient operating mode for the turbine) to absorb power variations caused by the cyclical nature of renewable energy sources such as wind turbines and PVs. This group modeled the microgrid using Simulink code which allows each component to be represented with all associated control feedback paths. These models incorporated feedback control sensors to determine the effectiveness of the fluctuation control system. They used a dynamic load model based on field data (see (Michigami 2002)) to simulate the fluctuations seen by the load in an islanded microgrid. This type of modeling is valuable for determining the effects of adding systems to the microgrid.

Oliva et al. (2003) performed a field study to examine the effect of a PV power generation station on the local grid. They looked at harmonics and whether or not any of them exceeded the Institute of Electrical and Electronics Engineers (IEEE) standards (IEEE 519-1992) for harmonic control in an electrical power system. Their test also covered several other issues associated with power quality.

Kakigano et al.(2008) propose a direct current (DC) microgrid configuration and converter control methods for generation and energy storage. Most of the distributed generation sources and energy storage devices are DC in nature (Such as PV arrays and batteries). Connecting these systems to a DC grid is advantageous since it would eliminate the AC distortion challenges associated with synchronizing AC inverters to the grid. The design would provide high quality DC power to the vast amount of DC devices (Especially electronics such as computers, etc.). The system would have AC inverters in the field close to the consumer as well as DC service. Fluctuation mitigation techniques and fault protection would be easier to implement in a DC grid environment. This paper provides a schematic of how the system would be implemented, complete with voltage levels, equipment placement, and simulation results.

Sharaf et al. (2008) propose a novel voltage source converter (VSC)-based hybrid power filter compensator (HPFC) scheme for effective reactive power compensation and harmonic reduction in distribution grid networks.

Balda et al. (Balda 2003) investigate the results of a power quality study performed on a PV generator in order to estimate the effects that inverter interfaced PV dispersed generation might have upon the quality of electric power. They measure a solar PV array in Texas for compliance with the IEEE's standard for harmonic distortion control in electric power systems (IEEE 519-1992). This paper also evaluates compliance with current harmonic distortion limits.

Braun (2008) evaluates the reactive power capabilities of distributed generators such as PV, wind systems, Bio-Gas, etc. Reactive power can be used to control voltage on the grid as a whole. The inverter tied to the grid is the device that will control the reactive power compensation seen by the grid. This paper looks at methods of optimizing reactive power control to the grid. This paper also gives an example of optimal reactive power allocation and an approach to decentralized voltage control making cost a key factor.

Engler et al. (2006) simulate inverter-controlled microgrids. Their work centers around the simulation results prepared using two rival software packages. The first of these is ATP-EMTP and the second is PowerFactory by DIgSILENT. Both packages allow the user to simulate transient effects in a microgrid or industrial system environment. They look at transient effects such as harmonics, fault analysis, transient spikes, optimal power flow, etc. This paper looks at the behavior of two or more grid forming inverters on the same grid environment and how voltage droop control techniques can allow this parallel operation. Another important piece of information is the advanced grid forming technique of varying the grids frequency according to the active power supply and varying the voltage based on the reactive power supply.

Braun et al. (2005) present their simulation results of a battery inverter in a software tool designed to analyze power flow in industrial systems. The purpose of this model is to demonstrate the control techniques necessary to control parallel inverters in an island or microgrid environment. The droop voltage and frequency control method described here allows multiple inverters to act as a grid forming device while load sharing with several other identical inverters. This control technique is outlined in a concept patented as Selfsync.

3. METHODS, ASSUMPTIONS, AND PROCEDURES

3.1. Test Site Location

All testing was conducted at Tyndall Air Force Base, in the Renewable Energy Tent City (RETC) facility. Figure 3 shows an aerial view of the testing facility.



Figure 3. Renewable Energy Tent City, Tyndall AFB

3.2. Test Equipment

The equipment used during testing is categorized into three grouped systems based on location and functionality. These systems comprise of the Component Panel Board, Data Acquisition Enclosure, and RETC Outdoor Equipment. Detailed specifications for all equipment can be found in Appendix A.

3.2.1. Component Panel Board Equipment

The component panel board is a custom-built mounting wall for critical components that may not be suitable for outdoor environmental conditions. The component panel board, housed in a controlled indoor climate located inside an Alaska Shelter System, consists of the Xantrex power system hardware, wiring, breakers, connections, and several pieces of measurement equipment that were used for data analysis. Not located on the component panel board but also located inside the Alaska Shelter System are the Deka/MK Unigy II Energy Storage System and a variable resistive AC load source for simulation of an environmental control unit (ECU). The manufacturer recommends this equipment be placed and protected inside a controlled indoor environment. The front and back side of the component panel board are shown in Figure 4 and Figure 5, respectively. The entire equipment list of the component panel board and additional equipment are listed in Table 1.



Figure 4. Component Panel Board (Front)



Figure 5. Component Panel Board (Back)

Table 1. Component Panel Board Equipment List

Equipment	Model-P/N	Quantity
Xantrex XW Hybrid Inverter/Charger	WX6048-120/240-60	3
Xantrex Solar Charge Controller	XW MPPT60-150	5
Xantrex Systems Control Panel	XW-SCP	1
Xantrex Automatic Gen Start	84-2064-00	1
Xantrex Communications Gateway	975-0330-01-01	1
Deka/MK Unigy II Energy Storage System	AVR-125-33	2
Eagle Power Solutions AC Load Bank	LB-60-30	1
Xantrex XW Power Distribution Panel	865-1015	2
CR Magnetics Transducers	CR5320-200	1
	CR5320-50	1
	CR210-400	1
	CR5210S-20	1
	CD5210-150	3
	CR2RL-1250	3
	CR5210-20	1

The Xantrex XW Hybrid Inverter/Charger is a true sine-wave, 120/240 VAC, initial split-phase inverter/charger incorporating a DC to AC inverter, battery charger, and AC auto-transfer switch designed for integrating renewable and energy storage applications into existing power systems. The AIPS program consists of three Xantrex XW Hybrid Inverter/Chargers reconfigured for single-phase monitoring and conditioning for each individual phase of 120/240 3-phase input with the capability of 6 kW of continuous output power for each unit. The inverters/chargers communicate their settings and activity through Xanbus, an integrated network communications protocol developed by Xantrex, via a Xantrex Systems Control Panel. A Xantrex XW Hybrid Inverter/Charger is illustrated in Figure 6.

The Xantrex XW Solar Charge Controllers are PV charge controllers designed to track the maximum power point of a PV array system, allowing for the maximum available current to charge an energy storage system. Using maximum power point tracking algorithms, the Xantrex

XW Solar Charge Controllers apply a variable load on the PV array until it finds the maximum wattage. At this point, the charge controllers hold the array for as long as the array continues to produce the maximum power possible. The solar charge controllers are able to regulate the PV array current and produce up to 3500 W and 60 A of charging current for charging of an energy storage system. The solar charge controllers are configured in a three-stage (bulk, absorption, and float) charging process, resulting in a more efficient charge compared to on-off relay type or constant voltage solid-state regulators. A Xantrex XW Solar Charge Controller is shown in Figure 7.



Figure 6. Xantrex XW Hybrid Inverter/Charger



Figure 7. Xantrex XW Solar Charge Controller

The Deka/MK Unigy II Energy Storage System is an interlocking, scalable, space saving absorbed glass mat (AGM) battery system composed of high energy density 125 A-hr, 4 V module lead acid battery cells. The system is connected in series to make a 2367 A-hr (C-20 discharge rate) battery system in a 48 V assembly capable of 355 A max current. The voltage, current, and amp-hour ratings are designed to provide the necessary energy storage capability for a 12.25 kW PV array system.



Figure 8. Deka/MK Unigy II Energy Storage System

3.2.2. Data Acquisition Enclosure Equipment

The data acquisition enclosure is a pass-through NEMA 3R vented enclosure between the SDC and PDP comprised of data hardware instrumentation, electrical equipment and electrical sensors to read and/or control gathered signals from voltage/current measurement sources or test equipment for storage, analysis, and operation. Additionally, the NEMA 3R enclosure, as illustrated in Figure 9, portably houses a panel PC for equipment monitoring, control, and communication between an array of system equipment and contactor relays for user control of a resistive load source for simulation of an ECU. A list of equipment housed inside the data acquisition enclosure is found in Table 2.



Figure 9. Data Acquisition Enclosure

Table 2. Data Acquisition Enclosure Equipment List

Equipment	Model-P/N	Quantity
NEMA Outdoor Enclosure	OD-50DDXC	1
National Instruments cRIO Hardware	NI-cRIO-9024	1
	NI-cRIO-9114	1
	NI-cRIO-9144	1
	NI-cRIO-9205	1
	NI-cRIO-9225	3
	NI-cRIO-9227	3
	NI-cRIO-9203	1
	NI-cRIO-9421	1
NI-cRIO-9474	1	
Unmanaged Ethernet Switch	NI-UES-3880	1
National Instruments Panel PC	NI-PPC-2015	1
Sola Power Supply	SDN-10-24-100P	1
Fuji IEC Contactor	SC-E5-24V	4
CR Magnetics Current Transformers	CR1ARL-760	6
CyberPower UPS	PR1500LCDRT2U	1

CompactRIO (cRIO), made by National Instruments (NI) for industrial control systems, is a reconfigurable embedded real-time control and acquisition system comprised of a real-time controller, reconfigurable I/O modules, a field-programmable gate array (FPGA) module, and an Ethernet expansion chassis for connection to a host PC. The NI CompactRIO was used as the sole data acquisition, processing, and control hardware for the Advanced Integrated Power Systems program. The used testing equipment and configuration is shown in Figure 10.

The NI cRIO-9024 real-time controller features an industrial 800 MHz Freescale processor with 512 MB DDR2 RAM and 4 GB of nonvolatile storage for deterministic, reliable data monitoring, logging, and control. The controller provides two Ethernet ports—10/100 and 10/100/1000—that conducts programmatic communication over a configured network. The real-time controller is connected to a NI-cRIO-9114. The NI-cRIO-9114 is an 8-slot reconfigurable embedded chassis that features a user-programmable Xilinx-Virtex 5-FPGA allowing high processing power with the ability to integrate hot swappable NI-cRIO I/O modules for data measurement and/or control from system sensors and equipment. A NI-cRIO-9144 EtherCAT slave chassis is used to add deterministic I/O capability through a daisy chain by means of CAT 5 Ethernet cabling to the National Instruments master controller. The addition of the NI-cRIO-9144 allows a maximum of sixteen I/O modules to be used for data measurement and control.

The I/O modules provide integrated analog or digital signal conditioning for system sensors and equipment to be utilized for data acquisition, monitoring, control, and analysis. The I/O modules vary in voltage and current signal ranges with an integrated wiring junction box and are hot swappable by connected directly to the NI-cRIO-9114 and Ni-cRIO-9144 chassis.

The NI-PPC-2015 National Instruments Panel PC, as shown in Figure 11 is a rugged industrial touch panel computer system that serves as a host PC and versatile measurement workstation to the CompactRIO hardware. The NI-PPC-2015 is equipped with a 2.0 GHz Pentium 4 processor with 512 MB DIMM RAM, a 40 GB hard drive, and Windows XP OS running National Instruments LabVIEW software for data acquisition and instrument control. The system offers connectivity to the NI-cRIO-9024 real-time controller through a 10/100 Ethernet I/O port.

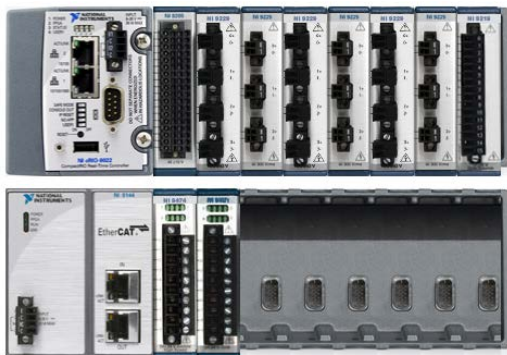


Figure 10. National Instruments cRIO Hardware



Figure 11. National Instruments Panel PC

Laboratory Virtual Instrumentation Engineering Workbench (LabVIEW) is program system software developed by NI featuring a graphical user display and program code for simulation,

data acquisition, instrument control, measurement analysis, and data representation from a range of I/O measurement signals. LabVIEW offers seamless connectivity with the NI cRIO measurement hardware and allows the user to visually represent measurement signals in a test system through a human-machine graphical user interface. A LabVIEW program, known as a Virtual Instrument (VI), was developed for the Advanced Integrated Power Systems program and is shown in Figure 12. The LabVIEW VI graphically shows the entire system design with all measured signals and controls used for test operation and data analysis.

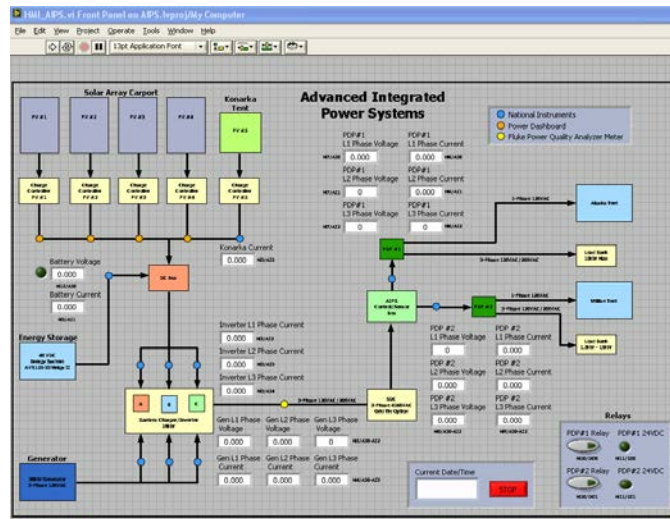


Figure 12. LabVIEW VI

3.2.3. RETC Outdoor Equipment

The RETC Outdoor Equipment comprises of the generator set, SDC, PDP, and PV array system. A component list is outlined in Table 3.

Table 3. Tent City Outdoor Equipment

Equipment	Model-P/N	Quantity
30 kW Generator Set	MEP-805A	1
SDC	SDC-1	1
PDP	PEU-156/E	1
PV Array System	SW 175	70
Utilis Shelter System	TM60	1
Konarka Thin Film Solar Panels	Power Series 40	60
Apogee Pyronometer	SP-110-L-46	8

The MEP-805A generator set is a brushless single bearing 3-phase mobile unit. The generator set consists of an engine, excitation system, speed governing system, fuel system, 24 VDC starting system, control system and safety fault system. The unit provides a 120/208 VAC at 104 A or 240/416 VAC at 52 A output voltage that is capable of supporting loads up to 30 kW. The generator is equipped with a 23-gal fuel tank requiring No. 2 diesel or JP-8, allowing

approximately eight hours of continuous operation at full load. The MEP-805A generator set is shown in Figure 13.

The SDC, shown in Figure 14, is a transformer and 150 kVA low-voltage load unit designed to accept primary power and reduce the voltage for power distribution. The unit receives 3-phase 3 wire delta electrical power at 2400/4160 VAC at 60 Hz, and transforms and distributes 120/208 VAC at 60 Hz, 60 A, 3-phase low voltage power. A dry type transformer, the SDC unit has one input source using three load break elbows while providing secondary output through sixteen 60 A cannon-type plugs. The primary power terminals are configured for a loop through double feed configuration. Additionally, the SDC has the capability to receive power from a smaller mission essential generator, such as the MEP-805A by bypassing the primary power and transformer through a low voltage cannon type plug to provide the necessary voltage for power distribution.



Figure 13. MEP-805A 30 kW Generator **Figure 14. Secondary Distribution Center (SDC)**

The PDP is a circuit breaker panel designed to distribute 1 and 3-phase low voltage electrical power from a 120/208 V AC power source such as a SDC into separate circuits for operation to system loads such as heating, ventilation and air conditioning (HVAC), lighting, and utility outlet systems capable of accepting loads up to 25 kW. Figure 15 shows the PDP used during testing. The 25 kW PDP has one 120/208 VAC, 60 A cannon plug input, one 120/208 VAC, 60 A cannon plug output, four 120 VAC, 20 A outputs, and one 120 VAC, 25 A convenience outlet.



Figure 15. Power Distribution Panel (PDP)

The PV array system shown in Figure 16 and Figure 17 consists of a 140 solar panel carport approximately 180 m², divided into two 70 panel sections located on the east and west side of the testing facility, respectively. Each section is further divided into four separate solar arrays. Each solar array outputs to a Xantrex XW MPPT60-150 Solar Charge Controller located on the component panel board. The PV array is equipped with Sunmodule SW 175 monocrystalline solar panels manufactured by SolarWorld providing a rated power of 175 W per panel with a rated current of 4.9 A and rated voltage of 35.8 V. The wiring configuration for one section of the PV array system is shown in Figure 18. Theoretically, this configuration should produce approximately 12.25 kW from each 70 panel section for a combined total of 24.5 kW. Due to sizing constraints of the inverters and solar charge controllers, one section divided into four arrays was used during testing to demonstrate solar renewable energy. To measure solar irradiance levels, three Apogee pyrometers were installed equidistant along the PV array system.



Figure 16. PV Array System Top



Figure 17. PV Array System Side

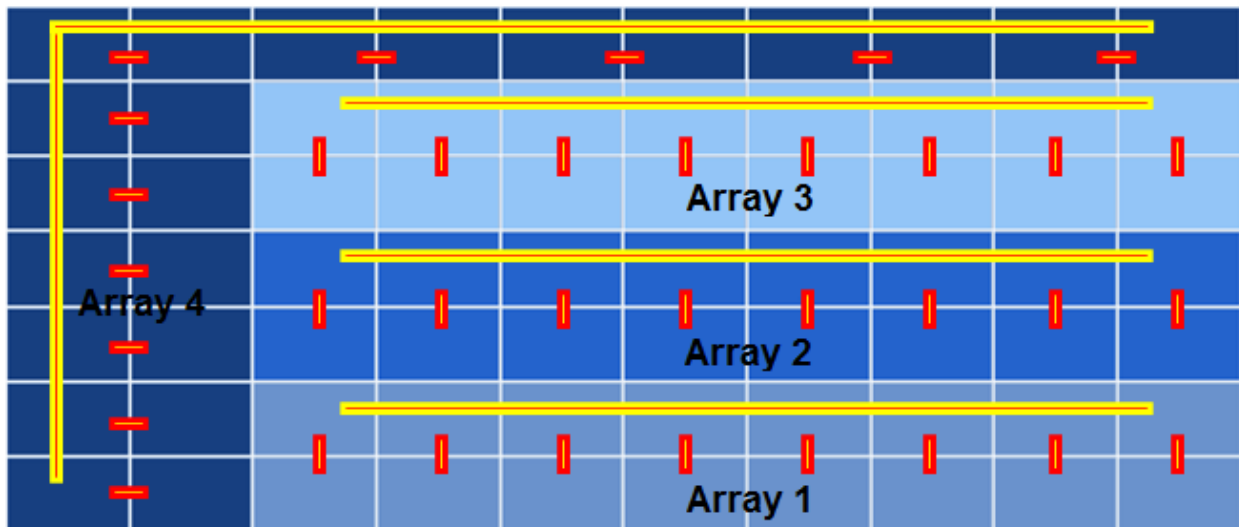


Figure 18. PV Array System Wiring

PV power generation was also provided by a 60 panel solar fly retrofitted to a TM60 Utilis shelter system. The PV array is equipped with Power Plastic 40 Series panels, provided by Konarka Technologies. Each panel is inserted in plastic sleeves affixed to the fly's mesh material via ultrasonic spot welds. Each panel measures 26.5 in \times 61 in, with an active area of 23.5 in \times 58.25 in (0.8831 m²) and a total active area of 52.99 m². The cells are arranged in 4 rows of 15, with each row along the faces of the standard fly. Figure 19 shows the Utilis shelter with the retrofitted Konarka panel solar fly.



Figure 19. Utilis Shelter with Konarka Panel Solar Fly

Electrically, 30 panels located on the east side of the tent were arranged with groups of 6 panels in series, and all of the groups interconnected in parallel. The same was done for the 30 panels located on the west side of the tent. Figure 20 diagrammatically shows how the east and west side panels are grouped. Each solar panel was wired directly to terminal boxes located at the South end of the tent (1 each for east and west sides). The series and parallel connections were made within the terminal box and outputted to a Xantrex XW MPPT60-150 Solar Charge Controller located on the component panel board. For solar irradiance measurement, one Apogee pyronometer was installed on each of the four faces of the solar fly. One Apogee pyronometer was also installed at the top of the solar fly.

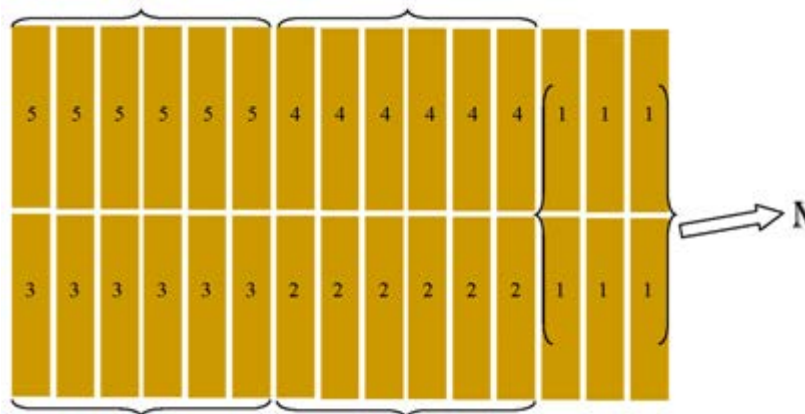


Figure 20. Konarka Panel Electrical Grouping

3.2.4. System Diagram

The diagram shown in Figure 21 provides a graphical representation of the overall system layout and integrated components for testing. For general maintenance, component checks, and repairs, the circuit diagram exhibited by Figure 22 details the electrical wiring and connections for the system. A set of complex cross referenced circuit diagrams are shown in Appendix B delineating all interconnected equipment and sensors to the data acquisition enclosure.

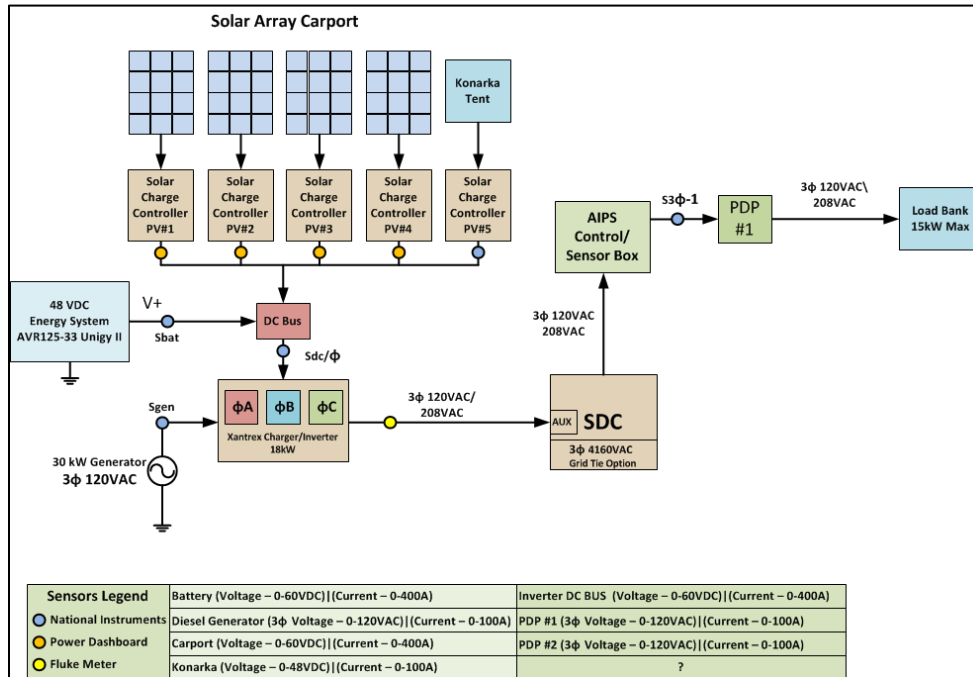


Figure 21. System Diagram

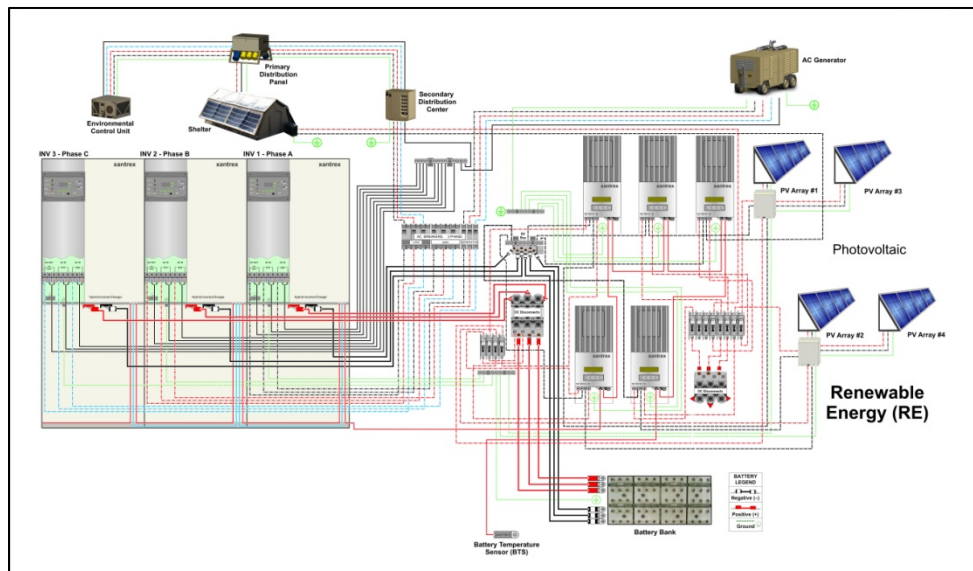


Figure 22. Electrical Connection of System

3.3. Test Procedures

Testing procedures were developed and performed based upon a list of sequential tasks and operations of the experiment that complied and coincided with AFRL directed safety test plans. Eight sets of testing were conducted according to these test procedures:

- Perform daily maintenance & system component check.
- Check safety equipment prior to each test run.
- Test data collection equipment.
- Prior to each test, brief all personnel on safety, specific capability being evaluated, and their role in the operation.
- Conduct tests according to established procedures and test matrix.
- Perform proper shutdown and storage of all equipment at the end of each test day.

3.3.1. Test Protocols

The experiment focused on determining the fuel savings potential through integration of renewable energy sources and on-site energy storage with a fully instrumented microgrid test bed. The experiment simulated an existing BEAR Base under standard current conditions, and compared the generator fuel required for the same load requirements with the addition of energy storage and renewable energy. For fuel savings analysis, the test was performed four ways:

1. Current System: The system simulated, as closely as possible, the operation of a BEAR Base for 24 hours under current conditions using a standard 30 kW MEP-805A generator set for power production.
2. Current System with Energy Storage: The second test added an energy storage system to the standard power hardware. The added storage would allow for excess energy production to be stored, and allow for the generator to be shut down when the storage system was fully charged.
3. Current System with Solar Panels and Energy Storage: The third test added both energy storage and renewable energy to the current system. This test would allow the generator to be shut down when the battery was fully charged while adding a renewable energy component with a peak rating near the peak power requirement for the simulated base.
4. Current System with Solar Panels: The fourth test evaluated the effectiveness of adding a large quantity of renewable energy through the use of solar panels into the current system without the integration of energy storage.

To provide a consistent, repeatable set of parameters to compare the different systems, the loads were simulated by programmed block schedules using a variable resistive load source. In this way, a true comparison can be performed, without concern for which test, for example, had a different ECU load due to different daily temperatures.

Two block schedules were developed, one for a high usage rate scenario and one for a lower usage rate scenario. In each load case, the typical daily usage was divided into three blocks: A low-load period of 8 hours representing the minimum usage periods (i.e. night time), a mid-load period of 12 hours representing morning and late afternoon usage, and a 4 hour high-load period representing peak usage. The block schedule is shown in Table 4.

Table 4. Load Block Schedule

Time (hr)	Load Scenario 1 (kW)	Load Scenario 2 (kW)
8	6	4
12	10	7
4	15	10

Each 24-hr block of testing was conducted over the course of several actual test days, with typically 6 hours of testing to be completed on each day. At the start of each day of testing, the 30 kW MEP-805A generator set was filled using No. 2 diesel fuel. The added fuel weight was recorded into a fuel data log; input as fuel consumed from the previous test run in the test matrix. To account for a simulated night, during tests where solar power was included in the system configuration, the solar energy was connected to the system for 12 hours, and disconnected for 12 hours. The solar was connected at the portions of the schedule representing daylight hours.

Each time the testing parameters were changed, the fuel tank was returned to full, and the weight required to fill it was recorded as part of the data for the previously test run in the matrix.

3.3.1.1. Current System Baseline Tests (System 1)

To evaluate the benefits and feasibility of integrating renewable energy into a current Air Force BEAR Base microgrid power system, baseline tests were conducted to establish initial metrics with respect to fuel consumption and various load block schedules. These baseline tests were implemented by using a 30 kW MEP-805A generator alone, without any use of integrated renewable energy and energy storage, to gather data on current fielded power generation systems. The test was run at both load block schedules. Table 5 and Table 6 show the detailed testing parameters for each system test and denote the date the test was conducted.

Note: Throughout the course of testing various power system configurations, the same high load and low load test matrices were used in order to evaluate the reduced fuel consumption compared to the “Current System Baseline Test” (generator only) when integrating renewable energy sources. However, the load profiles were rearranged during the tests of Systems 2 and 4 to better simulate the solar power output of the daylight hours in a complete 24-hr day.

Table 5. High Load—Baseline System Test Matrix

System 1 Load 1—Generator Only					
Test Number	Test Date	Test Start Time	Test Duration	Load	Power
			(hours)	(kW)	(kWh)
1	Mon, 26 Mar 2012	8:00	6	6	36
2	Tue, 27 Mar 2012	7:37	2	6	12
3	Tue, 27 Mar 2012	9:46	4	15	60
4	Wed, 28 Mar 2012	7:35	6	10	60
5	Thu, 29 Mar 2012	11:40	2	10	20
6	Fri, 30 Mar 2012	6:23	4	10	40

Table 6. Low Load - Baseline System Test Matrix

System 1 Load 2—Generator Only					
Test Number	Test Date	Test Start Time	Test Duration	Load	Power
			(hours)	(kW)	(kWh)
25	Mon, 26 Mar 2012	8:00	6	4	24
26	Tue, 27 Mar 2012	7:37	2	4	8
27	Tue, 27 Mar 2012	9:46	4	10	40
28	Wed, 28 Mar 2012	7:35	6	7	42
29	Thu, 29 Mar 2012	11:40	2	7	14
30	Fri, 30 Mar 2012	6:23	4	7	28

During the testing of System 1, Load Scenario 1 and System 1 Load Scenario 2, the electrical system was configured as shown in Figure 23. The 3-phase Xantrex Hybrid Charger/Inverter was bypassed, where only the MEP-805A Generator was connected and served as the sole power generation of the microgrid.

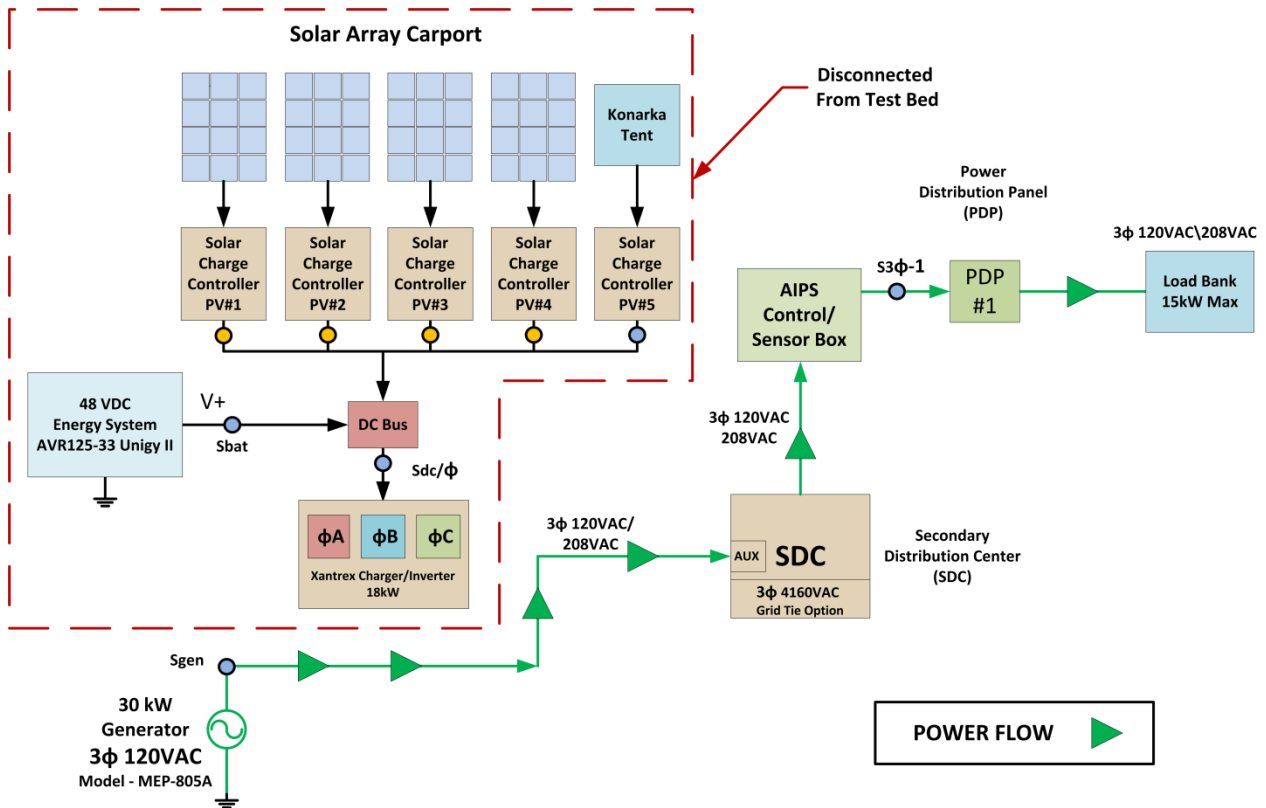


Figure 23. System 1 Test Configuration

The following test procedures were conducted in the sequential order during each test day:

1. The generator fuel supply was filled with No.2 diesel fuel to full capacity with a 5-gal fuel container. The weight of the fuel was recorded to a fuel log document in kilogram units.
2. Next, the load bank was preset for the power rating in Watts defined in the test block.
3. Then, the generator was turned on.
4. Immediately after the generator was turned on, the load was turned on by the LabVIEW VI, also known as the AIPS Controller. *Note:* Prior to the load being turned on the LabVIEW data logger was enabled to capture all of the necessary data of the system.
5. Once the duration of each test was successfully completed, the load bank and the generator were simultaneously turned off.
6. Subsequently, the LabVIEW data logger was disabled. The LabVIEW data log comprised of an excel spreadsheet, which included all the voltage and current sensor data in columns and time-stamped at a rate of 1 Hz.
7. At the end of each test, the same 5-gal fuel container was weighed before and after each refill. The fuel weight difference was recorded to a fuel log document to capture the amount of fuel that was consumed during each test. Refer to Figure 24 for an example of the fuel log document.
8. At the start of the next test day, the generator fuel supply was filled to full capacity as described in (step 1) to account for any fuel settling due to thermal effects.

AIPS Fuel Log						
Test #	Date	Time	Consumed Fuel Weight (lbs.)	Consumed Fuel Weight (kg)	Notes	kWhr
1	Mon - 26 Mar 2012	8:00	45	20.4	Filename: 03.26.2012 Test 1.xlsx	36
2	Tue - 27 Mar 2012	7:37	13.5	6.1	Filename: 03.27.2012 Test 2.xlsx	12
3	Tue - 27 Mar 2012	9:46	45.5	20.6	Filename: 03.27.2012 Test 3.xlsx	60
4	Wed - 28 Mar 2012	7:35	54	24.5	Filename: 03.28.2012 Test 4.xlsx	60
5	Thu - 29 Mar 2012	7:33	N/A	N/A	RERUN TEST	-----
6	Thu - 29 Mar 2012	9:45	N/A	N/A	RERUN TEST	-----
5	Thu - 29 Mar 2012	11:40	19.5	8.8	Filename: 03.29.2012 Test 5.xlsx	20

Figure 24. AIPS Fuel Log Data Example

3.3.1.2. Current System with Solar Panels Tests (System 4)

The purpose for System 4 tests was to evaluate the improved performance and fuel efficiency by integrating only solar energy without the availability of energy storage into the microgrid power system. The integration of the solar was tested in tests 21, 22, and 23 of Table 7 and tests 45, 46, and 47 of Table 8. All tests were based around local solar noon to acquire optimal performance during daylight hours. For instance, if the test duration lasted 2 hours, testing began an hour before solar noon of that particular day.

Note: Although this system is labeled as System 4, it is presented here out of sequence to reflect the order that the tests were actually run, as opposed to presenting the test procedures according to the arbitrary system numbers assigned prior to testing.

Tests 19, 20, and 24 of Table 7 and tests 43, 44, and 48 of Table 8 were baseline data taken from System 1 tests because the load rates were exactly same for those tests. For test system 4, these

tests represent the night time hours where there isn't any solar energy available and the primary power source is the generator.

Table 7. High Load - System with Solar Panels Test Matrix

System 4 Load 1—Solar Array & Generator					
Test Number	Test Date	Test Start Time	Test Duration	Load	Power
			(hours)	(kW)	(kWh)
19	Mon, 26 Mar 2012	8:00	6	6	36
20	Tue, 27 Mar 2012	7:37	2	6	12
21	Mon, 09 Apr 2012	10:43	4	15	60
22	Tue, 10 Apr 2012	9:43	6	10	60
23	Wed, 11 Apr 2012	11:42	2	10	20
24	Fri, 30 Mar 2012	6:23	4	10	40

Table 8. Low Load - System with Solar Panels Test Matrix

System 4 Load 2—Solar Array & Generator					
Test Number	Test Date	Test Start Time	Test Duration	Load	Power
			(hours)	(kW)	(kWh)
43	Mon, 26 Mar 2012	8:00	6	4	24
44	Tue, 27 Mar 2012	7:37	2	4	8
45	Thu, 12 Apr 2012	10:44	4	10	40
46	Fri, 12 Apr 2012	9:42	6	7	42
47	Mon, 16 Apr 2012	11:41	2	7	14
48	Fri, 30 Mar 2012	6:23	4	7	28

Figure 25 illustrates the electrical connections of the microgrid test bed for System 4.

The test procedures were conducted exactly as indicated in Section 3.3.1.1. The assumption was made that there were 12 hours of daylight in the 24-hr block schedule, so only 12 hours of the tests integrated the use of the solar power. Each of the tests integrating the solar energy was started based upon the solar noon. This was implemented to get the optimal peak performance of the solar energy introduced into the grid. Thus, the time each test started, the solar noon was targeted to occur halfway during the duration of the test.

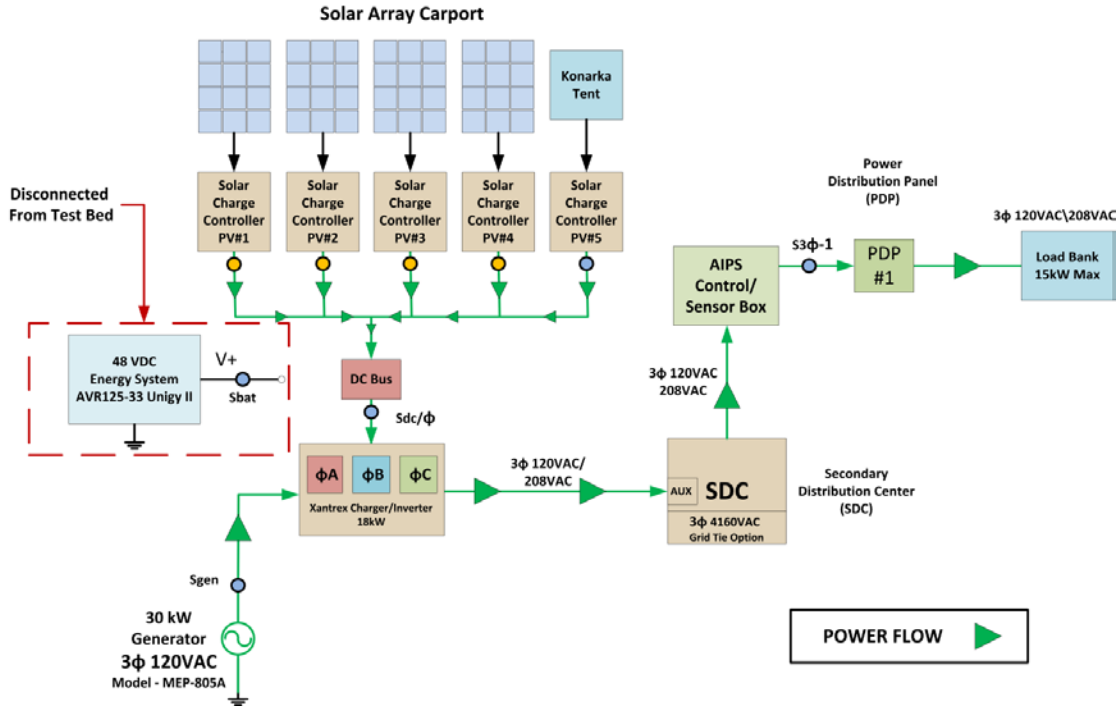


Figure 25. System 4 Test Configuration

3.3.1.3. System with Energy Storage Test (System 2)

System 2 was tested by integrating only energy storage into the microgrid test system. The objective was to evaluate the performance and fuel efficiency of the microgrid with integrated energy storage as compared to the integration of only solar power. Details of the test schedule are shown in Table 9 and Table 10 for each load case.

Table 9. High Load - System with Energy Storage Test Matrix

System 2 Load 1—Energy Storage & Generator					
Test Number	Test Date	Test Start Time	Test Duration	Load	Power
			(hours)	(kW)	(kWh)
7	Mon, 14 May 2012	6:34	6	6	36
8	Mon, 14 May 2012	12:35	2	6	12
9	Mon, 14 May 2012	2:35	4	15	60
10	Tue, 15 May 2012	4:47	6	10	60
11	Tue, 15 May 2012	10:47	2	10	20
12	Tue, 15 May 2012	2:47	4	10	40

Table 10. Low Load - System with Energy Storage Test Matrix

System 2 Load 2—Energy Storage & Generator					
Test Number	Test Date	Test Start Time	Test Duration (hours)	Load (kW)	Power (kWh)
31	Thu, 17 May 2012	4:56	6	4	24
32	Thu, 17 May 2012	10:56	2	4	8
33	Thu, 17 May 2012	12:56	4	10	40
34	Fri, 18 May 2012	4:33	6	7	42
35	Fri, 18 May 2012	10:33	2	7	14
36	Fri, 18 May 2012	12:33	4	7	28

For this test configuration, the AVR125-33 Unigy II Energy Storage system was connected to input of the 48VDC voltage bus of the Xantrex hybrid charger/inverter, while all of the solar power was disconnected. The MEP-805A diesel generator remained connected the same as the electrical connection described in System 4. Figure 26 illustrates the electrical system connections of System 2 test configurations implementing the use of only the Energy Storage and a MEP-805A Generator. An additional icon named “Charge Flow” indicates the direction of the current flow, while the AVR125-33 Unigy II Energy Storage system is being recharged. Throughout System 2 tests, the MEP-805A would charge the energy storage system when it required recharging as well as supply power to the load. Conversely, the routing of the current “Charge Flow” to the energy storage system is different and varies when integrated with the solar power depending on the load power rate and the solar power available. Further explanation is discussed in Section 3.3.1.4.

Before testing System 2, the AVR125-33 Unigy II Energy Storage system was charged to an equalized state, also known as equalization. This process is required for lead acid battery chemistries and the manufacturer recommended performing an equalization charge every 90 days to preserve the life of the battery. Thus far, this process was implemented in order to accurately test the energy storage system and determine it was at 100 percent capacity.

During the both tests for Systems 2, 12-hour blocks were conducted as denoted in Table 9 and Table 10, respectively. Refer to Figure 27 for a 24-hr load profile example (Load Scenario 1), which was used to model the power usage throughout a typical 24-hr day. Also, this load profile remained the same for Load Scenario 2, modified such that the loads match accordingly (4, 7 and 10 kW vs. 6 10 and 15 kW). *Note:* These test sequences were also used for System 3. For these two systems, the order of testing was important as each sequence of testing affected the remaining charge in the battery at the beginning of the next test sequence. For Systems 1 and 4, test sequence was irrelevant as there was no battery in the system. For that reason, for Systems 1 and 4, the tests were sequenced by load to improve testing efficiency.

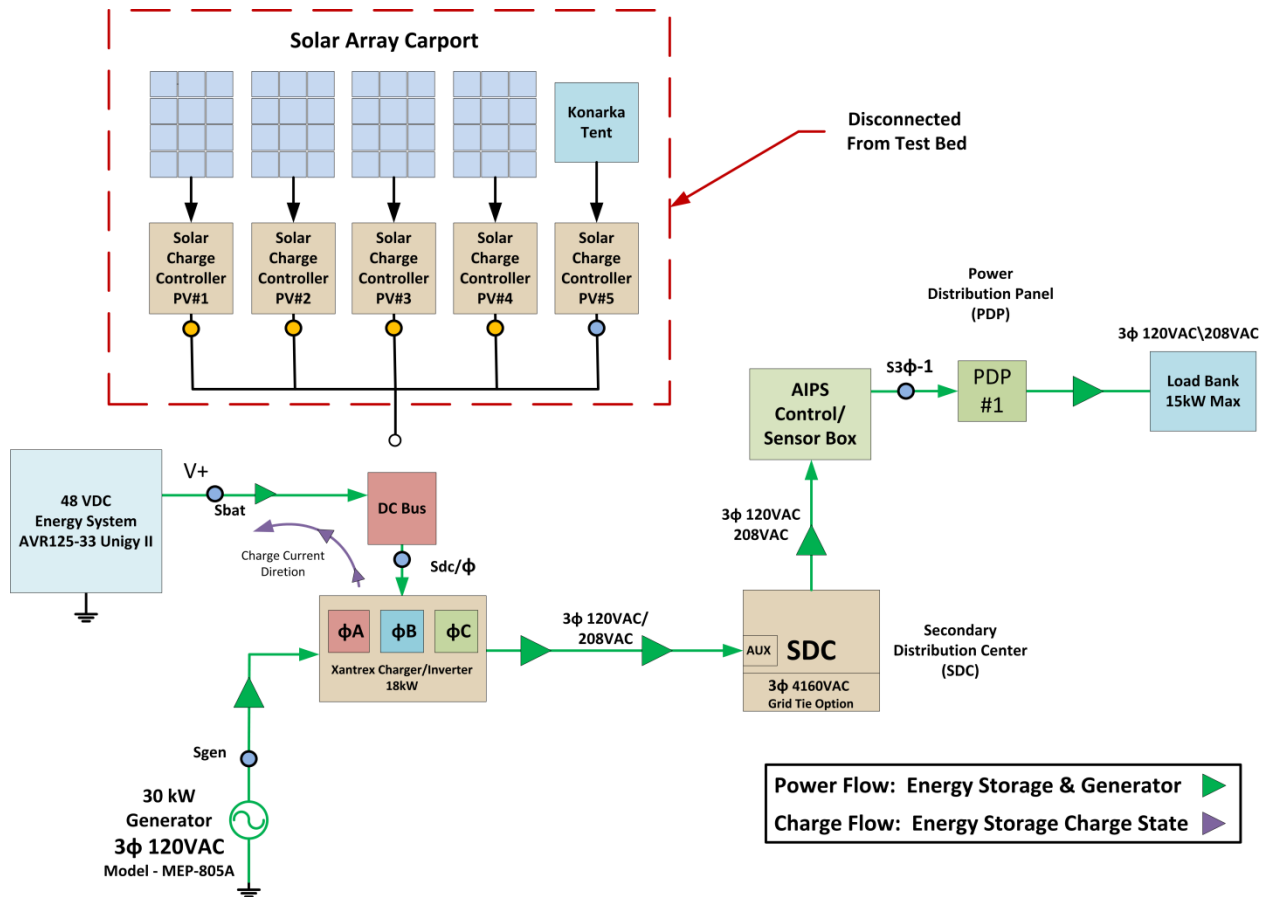


Figure 26. System 2 Test Configuration

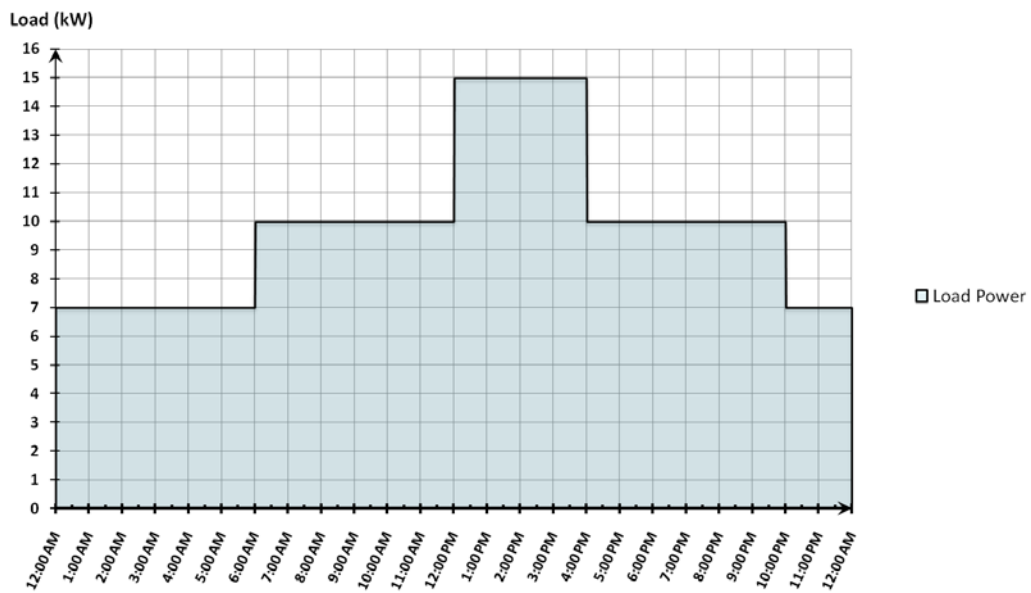


Figure 27. System 2 and 3 Load Sequence Example for a 24-hr Period

The following test procedures were conducted on the initial day of the first test beginning with System 2:

1. The generator fuel supply was filled with No.2 diesel fuel to full capacity with a 5-gal fuel container. The weight of the fuel was recorded to a fuel log document in kilogram units.
2. Next, the load bank was preset for the power rating in Watts defined in the test block.
3. Only the Energy Storage System was enabled to supply the sole source of power to the system.
4. Immediately after the Energy Storage System was turned on, the load was turned on by the LabVIEW VI, also known as the AIPS Controller. *Note:* Prior to the load being turned on the LabVIEW data logger was enabled to capture all of the necessary data of the system.
5. The Energy Storage System served as the sole source of power and was discharged until the 10 percent depth of discharge (D.O.D) time limit was reached. The 10 percent D.O.D time rate was used based upon the manufacturer's recommendations, due to the energy storage system specifications and system application. *Note:* The 10 percent D.O.D time limit for the Energy Storage System was defined according to the load rate and the specifications provided by the manufacturer. Refer to Figure 28 for the graphed 10 percent D.O.D time constraints of the AVR125-33 Unigy II Energy Storage system.
6. Once the Energy Storage system discharged up to 10 percent of its capacity, the MEP-805A generator was kicked on. During this time, the generator would charge the energy storage and provide power to the load.
7. The generator ran until the energy storage charge state went into the float stage for approximately 15 minutes.
8. Then, the generator was turned off, while the energy storage was left online and served as the sole source of power to the microgrid.
9. Steps 3–8 were repeated throughout the complete duration of the test block.
10. Once the duration of each test was successfully completed, the load bank and power system (energy storage and generator, if on) were simultaneously turned off.
11. Subsequently, the LabVIEW data logger was disabled. The LabVIEW data log comprised of an excel spreadsheet, which included all the voltage and current sensor data in columns and time-stamped at a rate of 1 Hz.
12. At the end of each test, the same 5-gal fuel container was weighed before and after each refill. The fuel weight difference was recorded to a fuel log document to capture the amount of fuel that was consumed during each test.

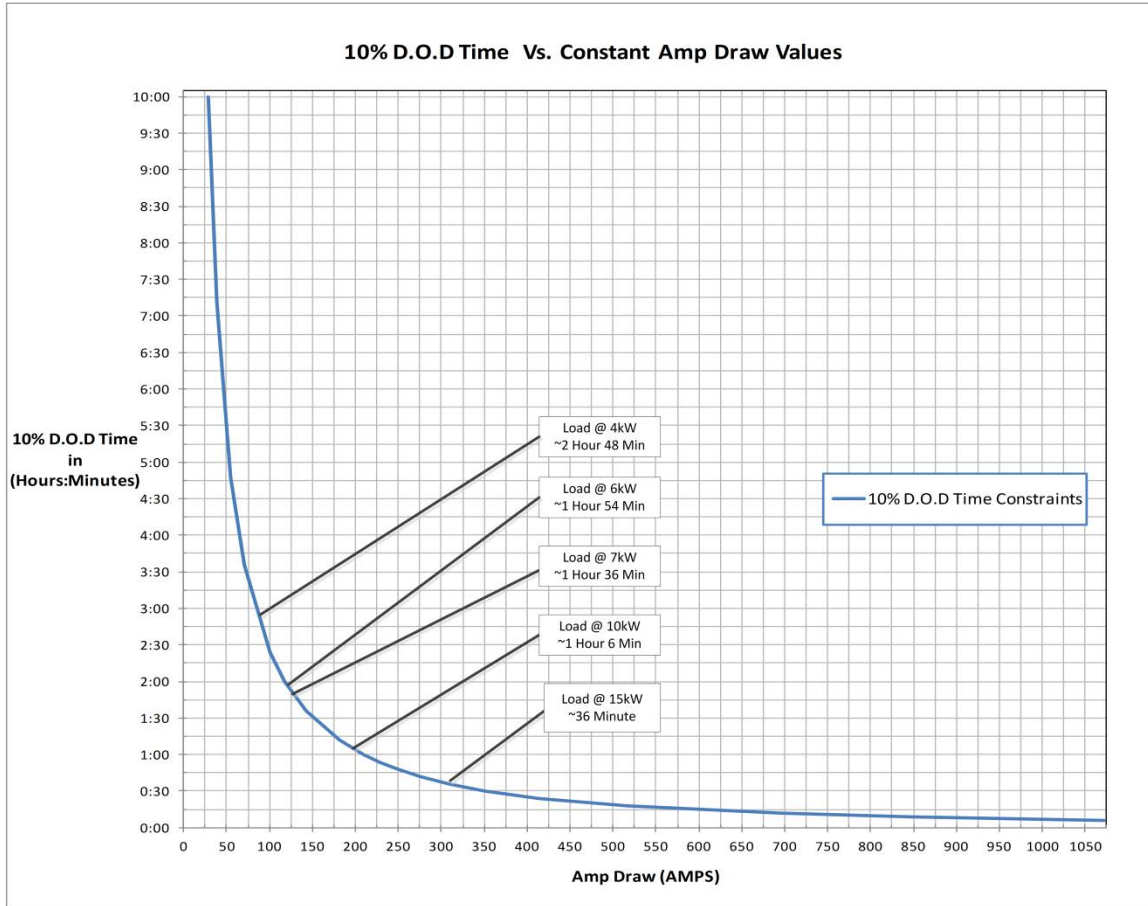


Figure 28. 10 percent D.O.D Time Limits for Energy Storage Power Supply

All of the test procedures were followed for the subsequent test days, except testing could start with either step (3) or step (6) depending on the current state of the charge/discharge cycle of the Energy Storage system.

For instances where the load changed magnitude during a battery discharge cycle, the correct battery recharge time was calculated by taking the percentage of the capacity of the energy storage left from the previous D.O.D rate and multiplying it by the current D.O.D rate.

Calculation example:

At a constant 10 kW load draw, the energy storage system is able to power the microgrid for approximately 1 hour and 6 minutes (Figure 28). If the load changes to 15 kW after 30 minutes, 55 percent of the 10 percent D.O.D time limit would have been already consumed based upon this calculation:

$$\% \text{ Energy Storage Capacity} = \frac{10\% \text{ D.O.D time limit @ Load Rate} - \text{Consumption Time @ Load Rate}}{10\% \text{ D.O.D time limit @ Load Rate}}$$

$$\% \text{ Energy Storage Capacity} = \frac{1 \text{ hour } 6 \text{ minutes} - 30 \text{ minutes}}{1 \text{ hour } 6 \text{ minutes}}$$

$$\% \text{ Energy Storage Capacity} \approx 55\%$$

Thus, the amount of time left to reach the 10 percent D.O.D. time limit for the remaining 15 kW load is 55 percent of the 10 percent D.O.D. time limit at the 15 kW load draw. Below is the calculation:

$$\text{New 10\% D.O.D time limit} = \% \text{ Energy Storage Capacity} * 10 \% \text{ D.O.D time limit @ Load Rate}$$

$$\text{New 10\% D.O.D time limit} = 55\% * 36 \text{ minutes}$$

$$\text{New 10\% D.O.D time limit} \approx 20 \text{ minutes}$$

Furthermore, the MEP-805A generator would be required to be turned on after a total of 50 minutes if the energy storage was on alone during a time period of 30 minutes at 10 kW and 20 minutes at 15 kW.

In amp hours, this equates to approximately 208 A-hr, which is around 10 percent of the 2000 A-hr capacity of the energy storage system. This corresponds to the 10 percent D.O.D. time limit rate. An important note to recognize is that, depending upon the discharge rate of the energy storage, the 10 percent D.O.D rate changes, but it is not proportional. For instance, if there is constant load of 325 A, the energy storage can only provide up to 30 minutes of power before recharging is required, which is only a total of approximately 162.5 A-hr. However, if there is a constant amp draw load of 50 A, the energy storage can provide up to 5 hours of power before recharging is required, which is a total of approximately 250 A-hr. Thus, the rate at which the energy storage discharges affects its overall performance and D.O.D time limits as well as the A-hr rate. This should be taken into account when designing microgrid power systems that use renewable energy sources, especially where load rates are constantly changing. Further discussion to optimize this design is discussed in Section 3.3.1.4.

3.3.1.4. System with Solar and Energy Storage Test (System 3)

The last microgrid configuration tested was System 3. These test systems comprised of the complete integration of the solar, energy storage, and generator to supply power to the microgrid. The purpose of this test was to evaluate the improved performance and fuel efficiency against the other microgrid configurations. Details of the test schedule are shown in Table 11 and Table 12 for the two load profiles.

Table 11. High Load - Current System with Solar and Energy Storage Test Matrix

System 3 Load 1—Generator, Solar Array, & Energy Storage					
Test Number	Test Date	Test Start Time	Test Duration (hours)	Load (kW)	Power (kWh)
13	Wed, 30 May 2012	6:40	6	6	36
14	Thu, 31 May 2012	6:38	6	10	60
15	Thu, 31 May 2012	10:38	4	15	60
16	Thu, 31 May 2012	12:38	2	10	20
17	Fri, 01 Jun 2012	7:05	4	10	40
18	Fri, 01 Jun 2012	9:05	2	6	12

Table 12. Low Load - Current System with Solar and Energy Storage Test Matrix

System 3 Load 1—Generator, Solar Array, & Energy Storage					
Test Number	Test Date	Test Start Time	Test Duration (hours)	Load (kW)	Power (kWh)
37	Tue, 22 May 2012	9:06	6	4	24
38	Mon, 04 Jun 2012	6:38	6	7	42
39	Mon, 04 Jun 2012	10:38	4	10	40
40	Mon, 04 Jun 2012	12:38	2	7	14
41	Wed, 23 May 2012	7:49	4	7	28
42	Wed, 23 May ₂₀₁₂	11:49	2	4	8

For this test configuration, the AVR125-33 Unigy II energy storage system and all of the solar charge controller outputs (as described in Systems 2.1 and 2.2) were connected to input of the 48VDC voltage bus of the Xantrex hybrid charger/inverter. The MEP-805A diesel generator remained connected the same as the electrical connection described previously. Figure 29 illustrates the electrical system connections of System 3 test configuration, which implements the both solar power and energy storage. Note: Figure 29 shows the power flow when all power sources are supplying power to the load.

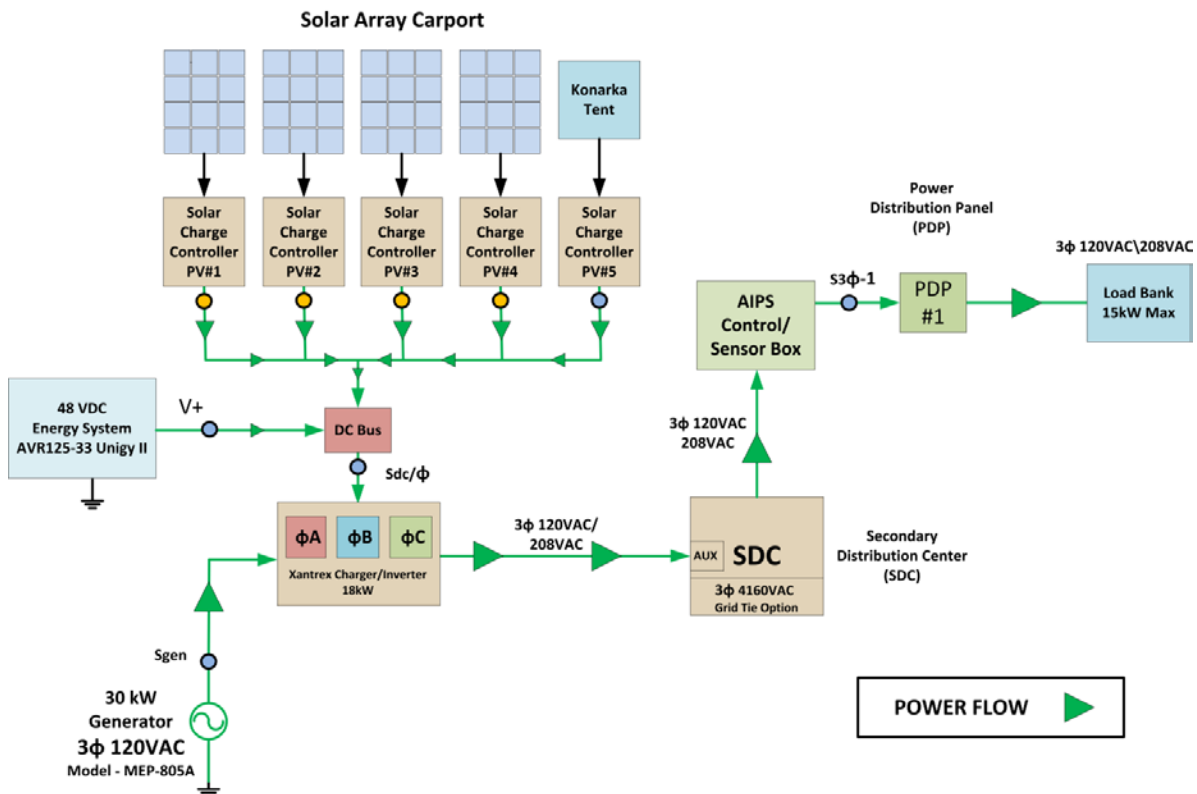


Figure 29. System 3 Test Configuration

Alternatively, there are two possible cases that can occur when the energy storage is being recharged. The first case, illustrated in Figure 30, shows the energy storage being recharged by both the MEP-805A generator and the solar power. This occurs when there is excessive energy available from the generator. The excess energy is then routed back through the inverter and onto the 48 VDC voltage bus. If there is also available solar power, the power from the solar will merge with the generator power in order to recharge the energy storage. The solar power is routed from the solar charge controllers. Additionally, during the charge cycle the Xantrex smart controller monitors and controls all available power fed into the system by both the Xantrex hybrid inverter/charger and solar charge controllers. Moreover, the energy storage will accept any available power there is in order to properly recharge at the most efficient rate.

It is noted that the maximum power output of the Xantrex hybrid inverter/charger is only 18 kW continuous output power, while the MEP-805A generator maximum output power is 30 kW. This limits the amount of power which can be utilized for charging the battery. For example, during the tests when the microgrid was loaded at 15 kW, only 3 kW were available to recharge the energy storage. Likewise, at the 10 kW load, only 8 kW was available to recharge the energy storage. Therefore, the time to recharge the energy storage during such conditions was prolonged, and energy was wasted. If the generator and Xantrex inverter were matched to the same specifications, the power use could be maximized, optimizing the microgrid performance during the charge cycle of the energy storage which would increase the fuel efficiency of the microgrid test system.

In contrast, when there is solar power available while the energy storage is being recharged, the excess amount of power supplied from the generator output of the Xantrex hybrid inverter/charger and the addition of the available solar charge controllers power output serve as an aggregate amount of power used to charge the energy storage system. For instance, when the max load of 15 kW is being consumed, the 3 kW available from the generator and the available solar power are routed to the input of the energy storage system. The solar charge controllers are limited by 3500 W and 60 A output per charge controller. The Xantrex Smart Controller also limits the rate of recharge of the Energy Storage System based on the input parameters programmed into the Xantrex bus controller.

Figure 31 illustrates the second case, where the total amount power produced by the generator is consumed by the load, and the available solar power is used to charge the energy storage system. This is possible, but this case never did exist in our test because the loads never exceeded the Xantrex hybrid inverter/charger output of 18 kW. At worst case scenario, there was 3 kW of power available from the generator, since the max load rate was set at 15 kW throughout the entirety of testing.

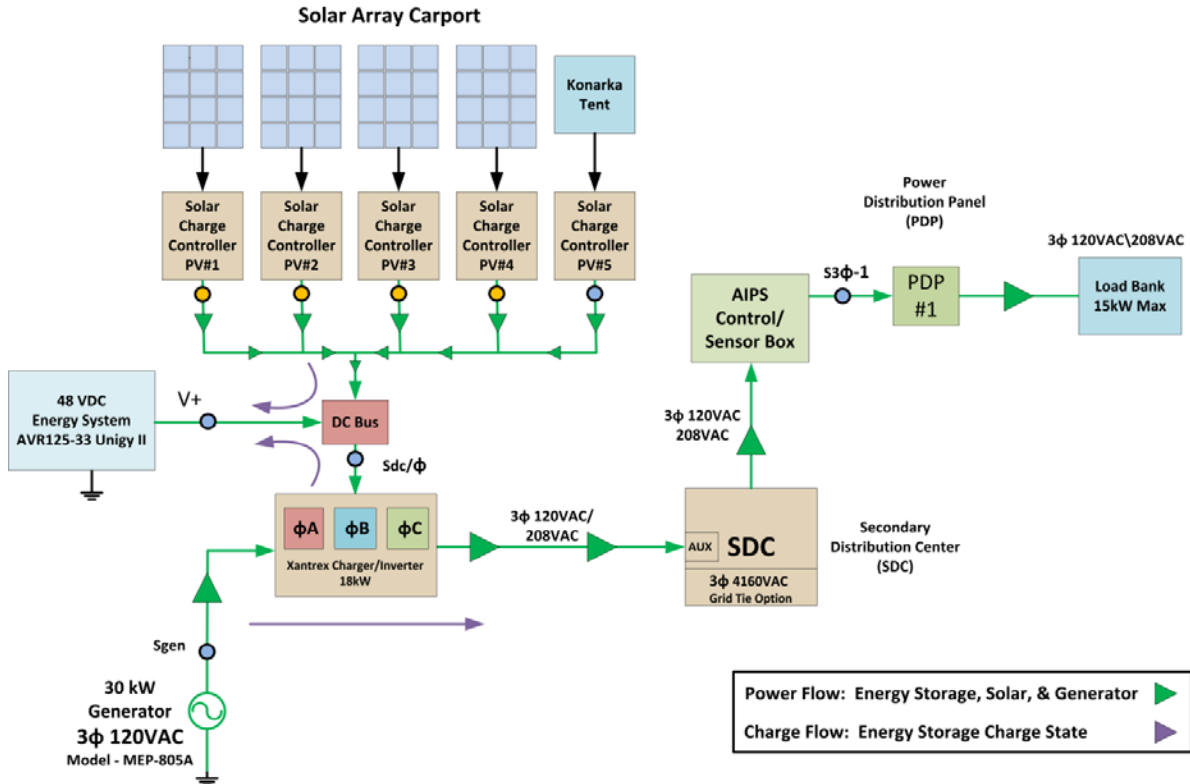


Figure 30. System 3 Energy Storage Charge State 1

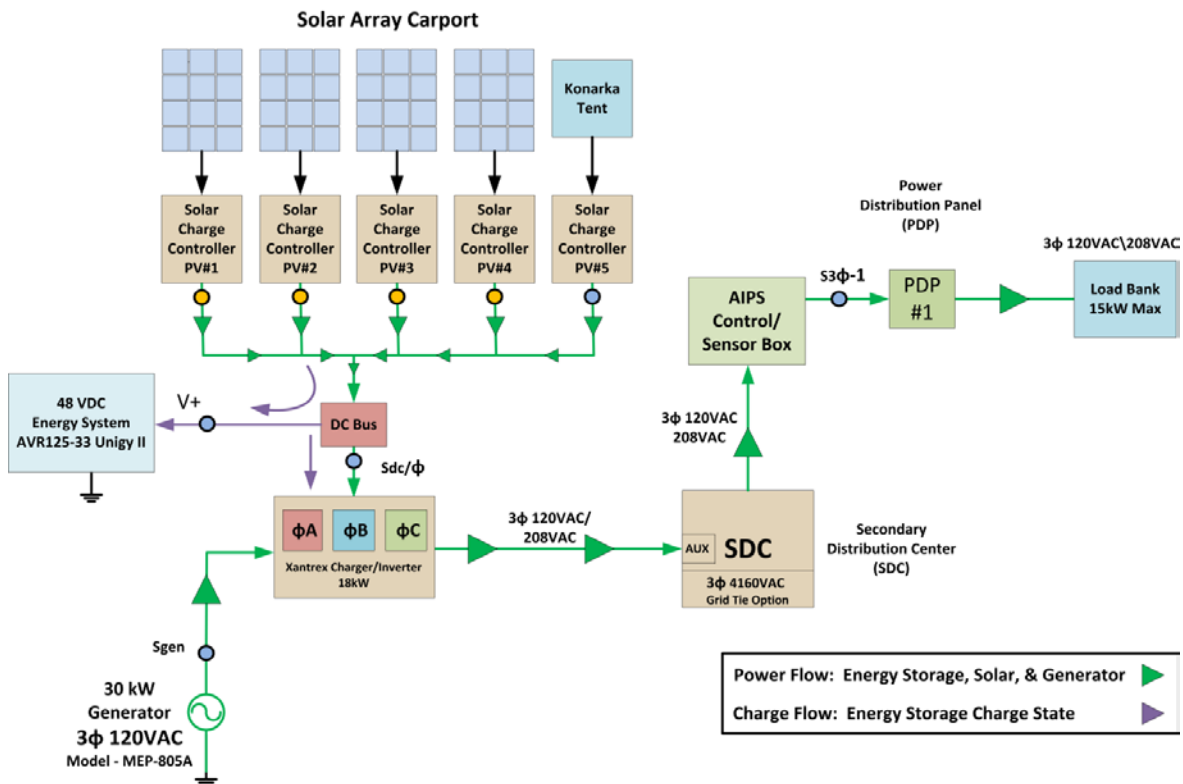


Figure 31. System 3 Energy Storage Charge State 2

The following test procedures were conducted on the initial day of first test beginning with System 3:

1. The generator fuel supply was filled with No.2 diesel fuel to full capacity with a 5-gal fuel container. The weight of the fuel was recorded to a fuel log document in kilogram units.
2. Next, the Load bank was preset for the power rating in Watts defined in the test block.
3. Only the Solar Power and Energy Storage System were enabled to supply the sole source of power to the system.
4. Immediately after step 3 the load was turned on by the LabVIEW VI, also known as the AIPS Controller. *Note:* Prior to the load being turned on the LabVIEW data logger was enabled to capture all of the necessary data of the system.
5. The Solar Power and the Energy Storage System served as the sole source of power and was discharged until the 10 percent D.O.D time limit was reached. The same 10 percent D.O.D time rate was used in the same method as the previous test Systems 2.
6. Once the Energy Storage system discharged up to 10 percent of its capacity, the MEP-805A generator was kicked on. During this time, the available generator and solar would charge the energy storage and provide power to the load.
7. The generator ran until the energy storage charge state went into the float stage for approximately 15 minutes.
8. Then, the generator was turned off, while the solar charge controllers and energy storage was left online and served as the sole source of power to the microgrid.
9. Steps 3–8 were repeated throughout the complete duration of the test block.
10. Once the duration of each test was successfully completed, the load bank and power system (energy storage and generator, if on) were simultaneously turned off.
11. Subsequently, the LabVIEW data logger was disabled. The LabVIEW data log comprised of an excel spreadsheet, which included all the voltage and current sensor data in columns and time-stamped at a rate of 1 Hz.
12. At the end of each test, the same 5-gal fuel container was weighed before and after each refill. The fuel weight difference was recorded to a fuel log document to capture the amount of fuel that was consumed during each test.

4. RESULTS AND DISCUSSION

4.1. Fuel Consumption

Since the primary goal of the present work is to determine the ability to save fuel in a deployed setting, the fuel consumed is the primary measure used here to compare the various tests. The fuel consumption for each test is shown in Table 13.

Table 13. Fuel Consumption Comparison

System	Load Scenario 1		Load Scenario 2		Average Savings (%)
	Fuel (kg)	Savings vs. Baseline (%)	Fuel (kg)	Savings vs. Baseline (%)	
1 (Generator Only)	95.0		83.5		
2 (Generator + Battery)	79.0	16.8	58.2	30.3	23.6
3 (Generator + Battery + Solar)	59.2	37.7	43.4	48.0	42.9
4 (Generator + Solar)	93.9	1.2	79.6	4.7	2.9

Comparing the fuel consumption for the baseline configuration (generator only) between the two load cases, there is a 12 percent difference in fuel consumption. However, examination of the load profiles shows that the energy consumption difference is 32 percent. This is a ratio of 2.7:1 comparing energy not consumed to fuel saved.

In addition to this work, the generator was run for a period of 6 hours without any load, which resulted in a consumption rate equivalent to 57.6 kg/day, or about 39 percent savings compared to the load-case 1 baseline. This shows that a program of energy conservation without modification of power production will result in minimal savings; even 100 percent elimination of all loads will only reduce fuel consumption by 39 percent if we do not change how the generators are operated.

4.2. Detailed Power Data

In addition to fuel consumption, detailed data was collected regarding the different portions of the system, as outlined in the methods section. The data presented in this section is the output of the LabVIEW data, collated to show as a continuous 24-hr block of time.

4.2.1. Data Calibration

During review of the data, it was observed that the current transducers attached to the output of the generator were not properly calibrated. After the completion of the testing, the transducers were calibrated to determine their actual behavior. Based on this recalibration, the previously collected data was modified by multiplying the measured results by the calibration curve. For the sake of completeness, the calibration curves used are shown here, in Figure 32. These graphs show the calibration ratio as a function of actual amps of current through the transducer for each phase of current. The calibration ratio is a ratio of the correct calibration divided by the as-used

calibration. This factor, then, gives the error in the collected data, with the error between approximately 5 and 25 percent (1.05–1.25). The error was in the direction of underreporting the current from the generator.

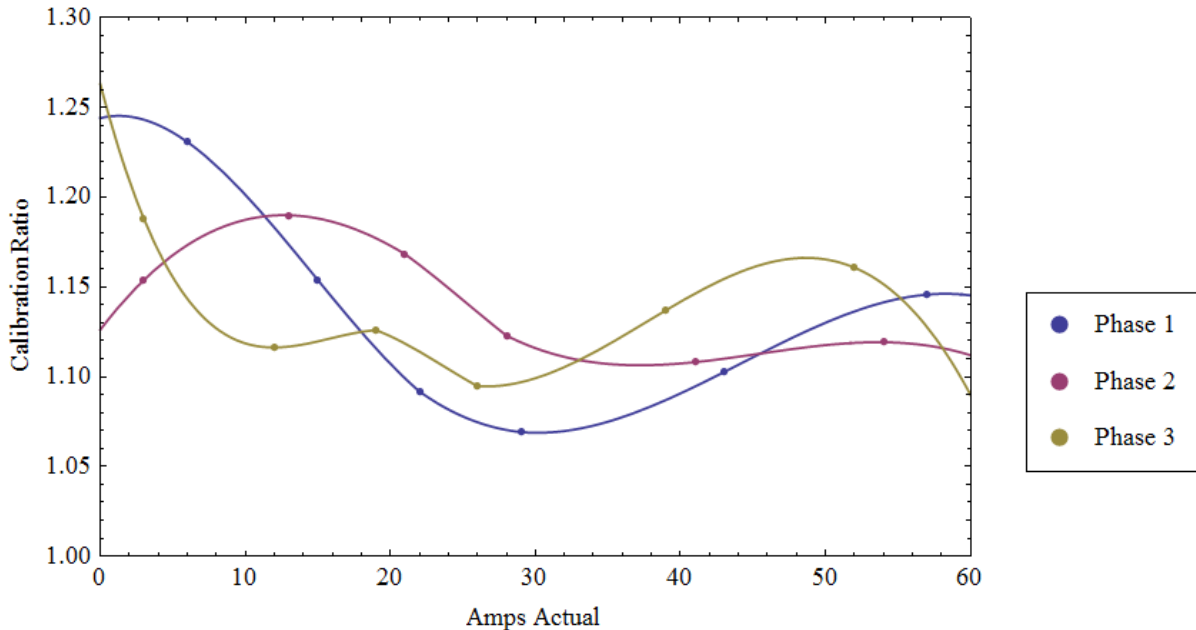


Figure 32. Calibration Curves

4.2.2. System Data

The output for System 1, Load Scenario 1 is presented in Figure 33. This is the baseline system with only the generator and the load in the circuit, and the load is the higher of the two levels. Only the power consumption of the applied load and generator output are displayed, as the solar system and battery are disconnected. The differences between the two curves can be attributed to transmission efficiency, and the results are consistent with expectations, indicating that our calibration curves are reasonable.

The output of System 2, Load Scenario 1 is shown in Figure 34. This is the baseline system with the addition of a battery. The generator was cycled on and off depending on the charge state of the battery. In the graph, a negative power for the battery system indicates that the battery is charging, while a positive value indicates that the battery is discharging.

The output of System 3, Load Scenario 1 is shown in Figure 35. This is the baseline system with the addition of a battery and solar power. The generator was cycled on and off depending on the charge state of the battery and availability of solar power. In the graph, a negative power for the battery system indicates that the battery is charging, while a positive value indicates that the battery is discharging. In this graph, the solar power indicated is the solar power which is actually added to the load, not the total available. When the generator is operating, the solar power does not cross the inverter and add in to the grid, because there is an excess of power already available from the generator. However, if the battery is not full, the solar power is used to charge the battery, even if the generator is also operating.

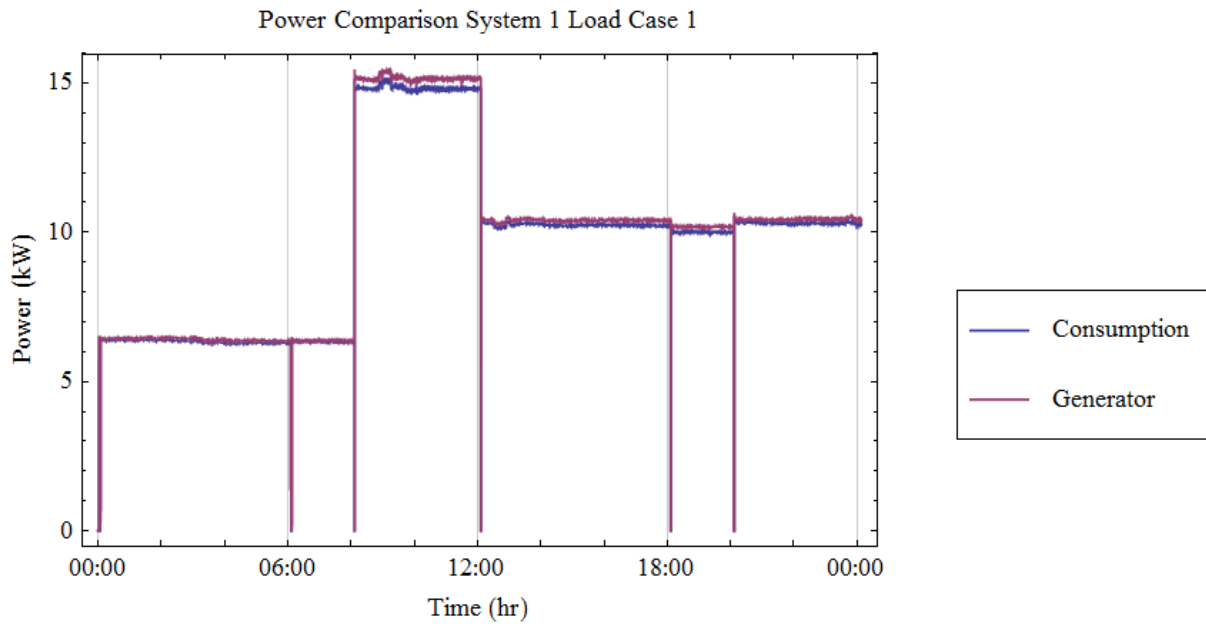


Figure 33. System 1/Load Scenario 1

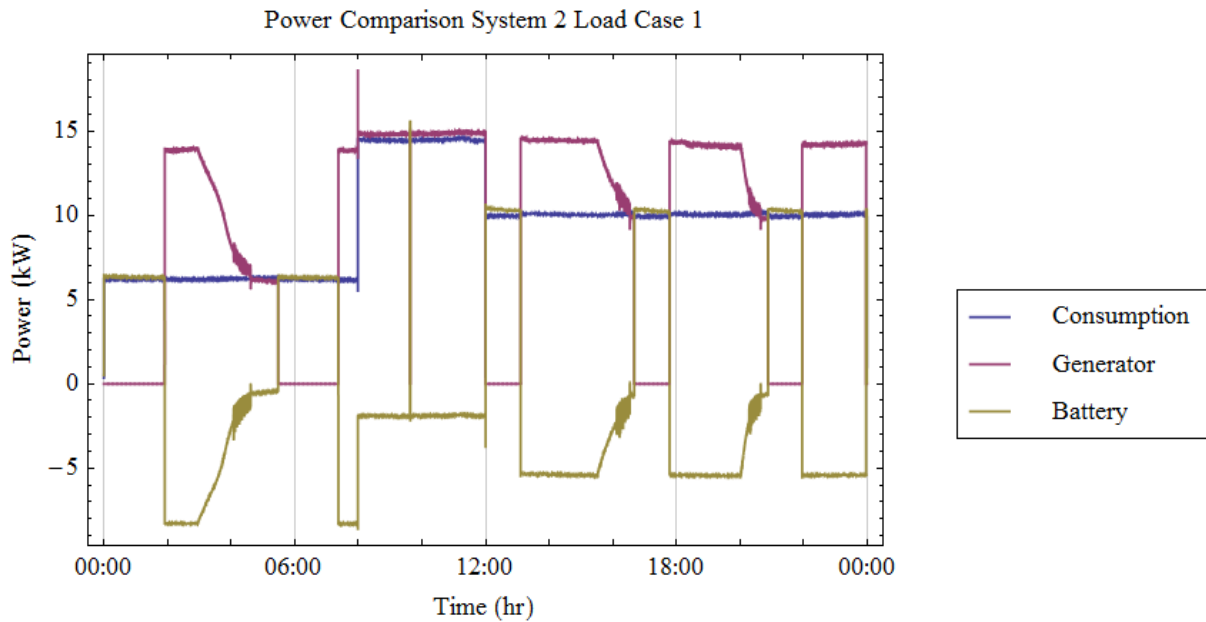


Figure 34. System 2/Load Scenario 1

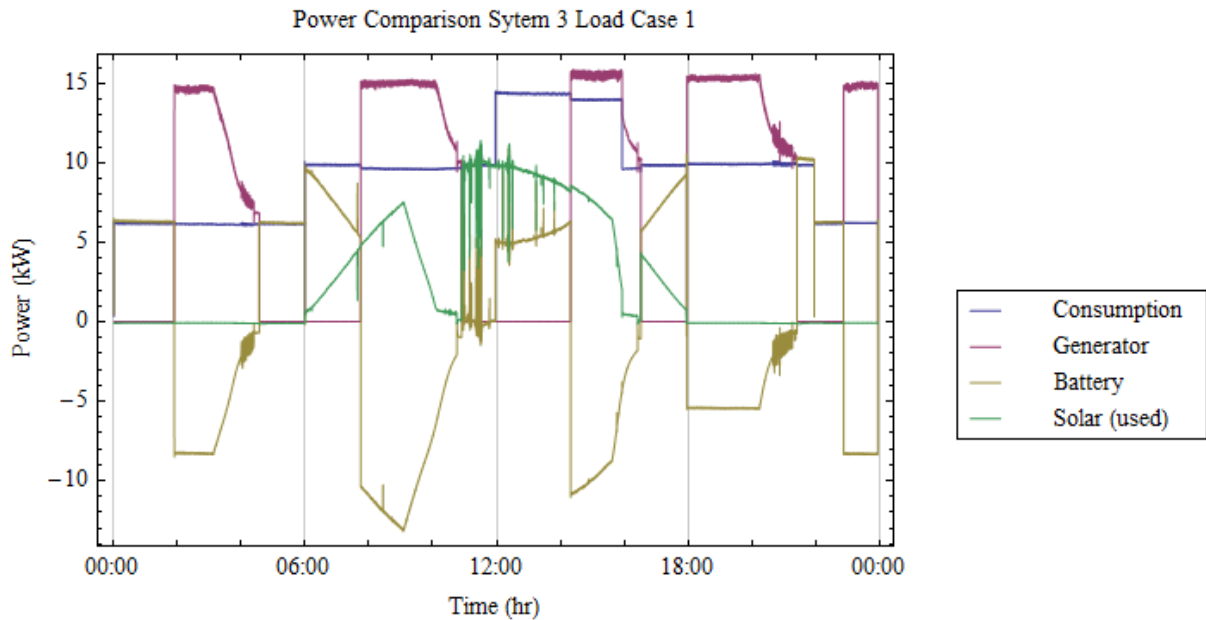


Figure 35. System 3/Load Scenario 1

Since the available solar power is not necessarily consumed, it is also instructive to observe the total solar power available vs. the actual power consumed. This is shown in Figure 36. To determine the available solar power, the solar irradiance was calculated by averaging the readings of the pyrometers distributed on the solar array, and this value was multiplied by the rated power output of the panels.

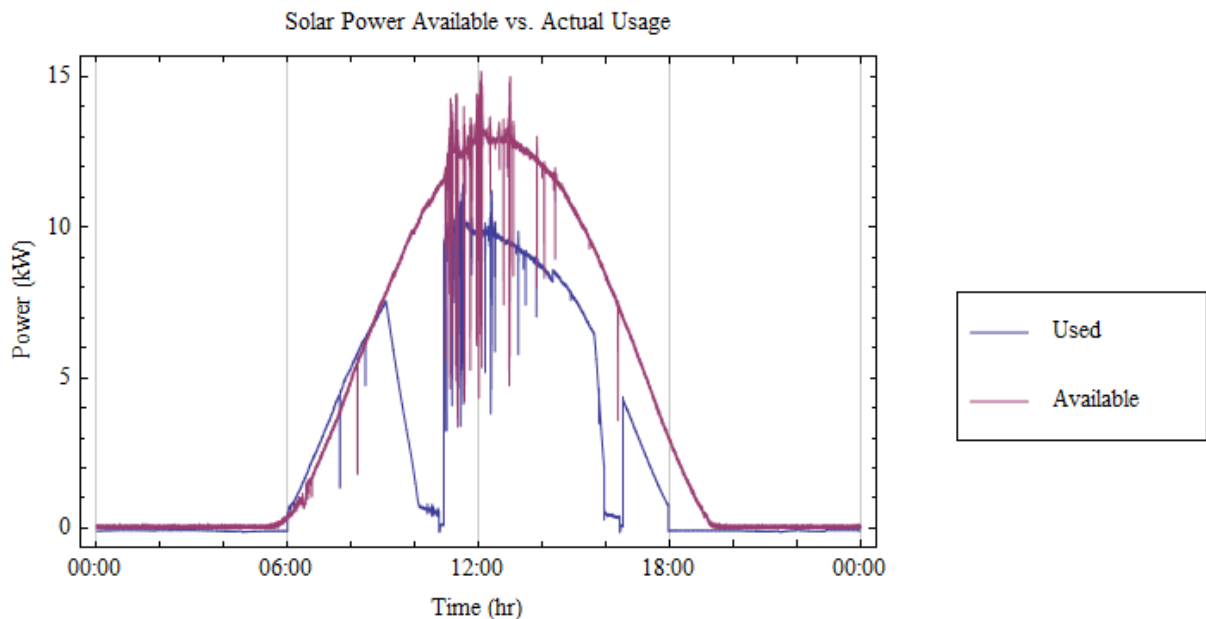


Figure 36. System 3/Load Scenario 1, Available vs. Used Solar Power

The output of System 4, Load Scenario 1 is shown in Figure 37. As can be observed in the graph, very little of the available solar energy was actually utilized. This is also reflected in the fuel consumption measurements. Since the generator was always running, the solar power was not needed.

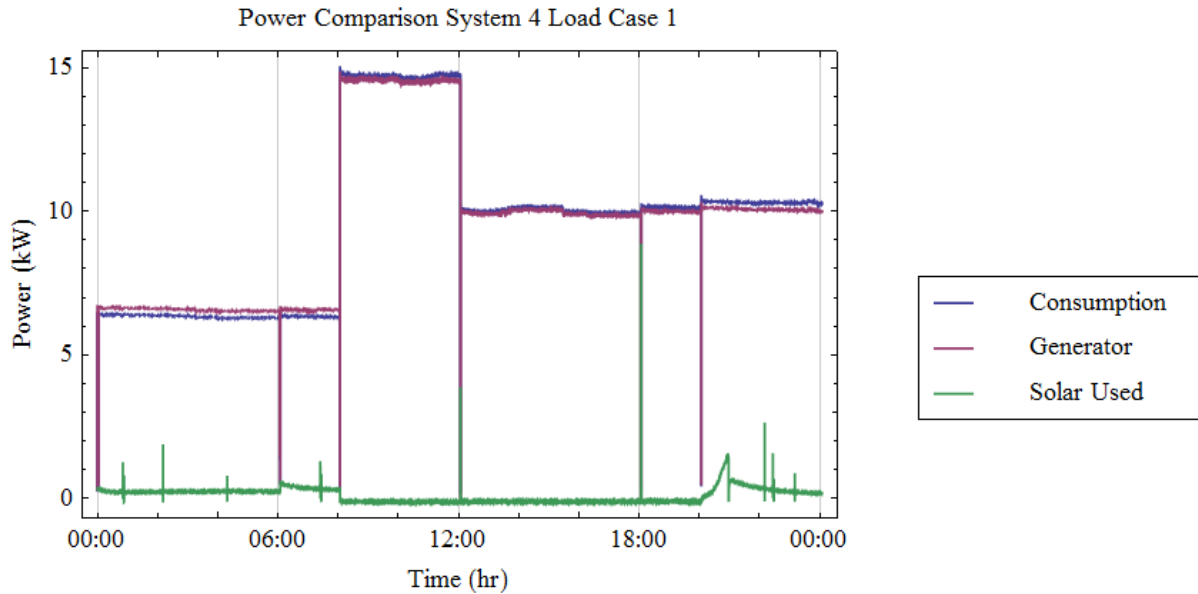


Figure 37. System 4/Load Scenario 1

In Figure 38, the data of System 4, Load Scenario 1 is again presented, but compared against available solar power. This graph shows that, while adequate solar power was generally available, reliance on solar power alone would have led to momentary power loss. Also, it can be observed that the data collection actually occurred over several days, with the testing centered around local solar noon to maximize the available solar energy. Even under these very favorable conditions, the solar power alone resulted in next to no net fuel savings.

The output of System 1, Load Scenario 2 is shown in Figure 39, while the output of System 2, Load Scenario 2 is shown in Figure 40. The output of System 3, Load Scenario 2 (showing actual solar power used) is shown in Figure 41. A comparison solar power used to solar power available for this test is shown in Figure 42, while the output of System 4, Load Scenario 2 is shown in Figure 43.

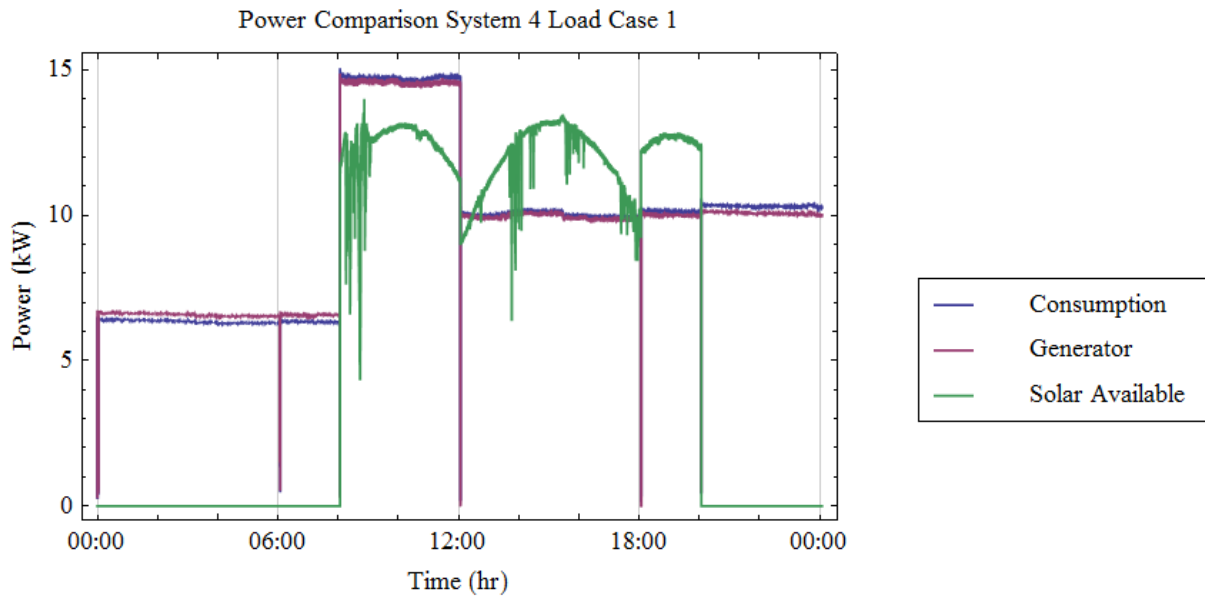


Figure 38. System 4/Load Scenario 1, Available Solar Power

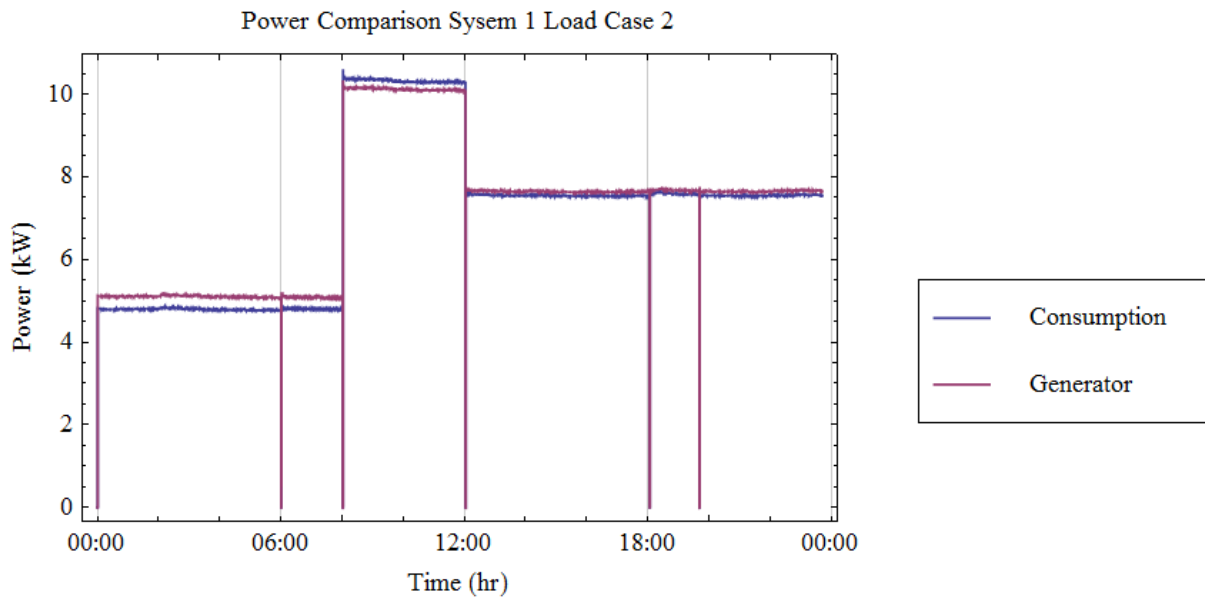


Figure 39. System 1/Load Scenario 2

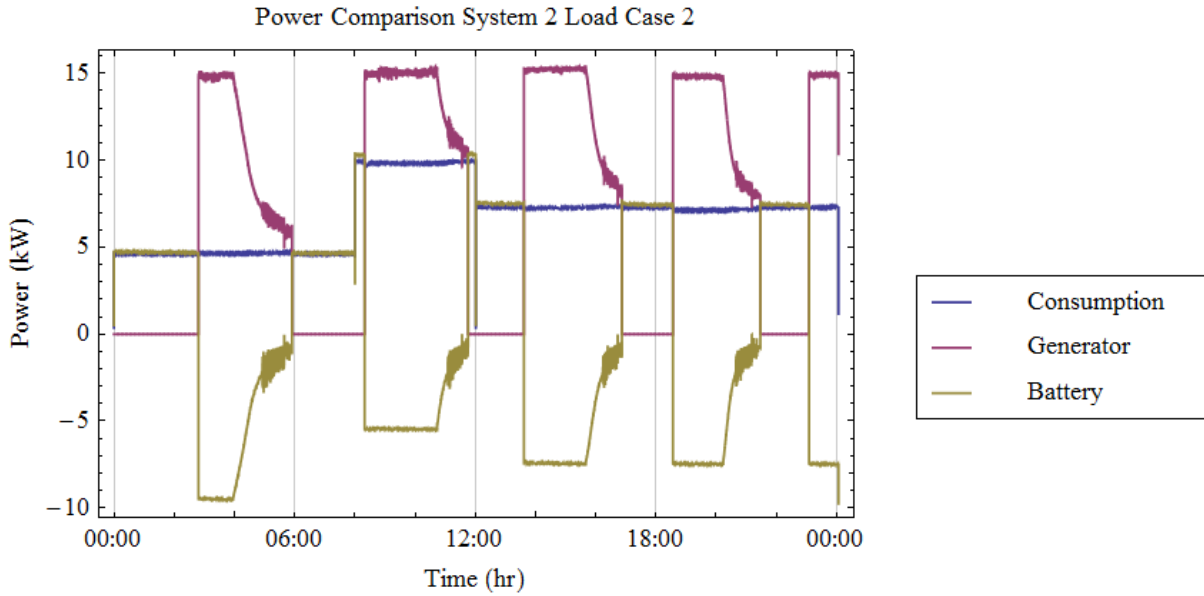


Figure 40. System 2/Load Scenario 2

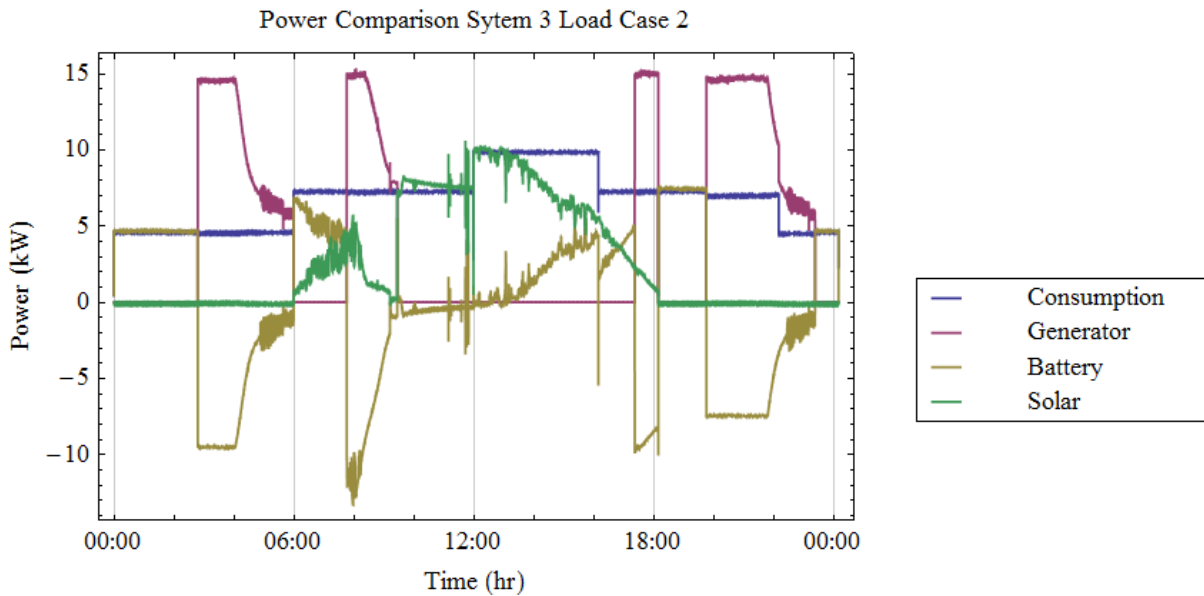


Figure 41. System 3/Load Scenario 2

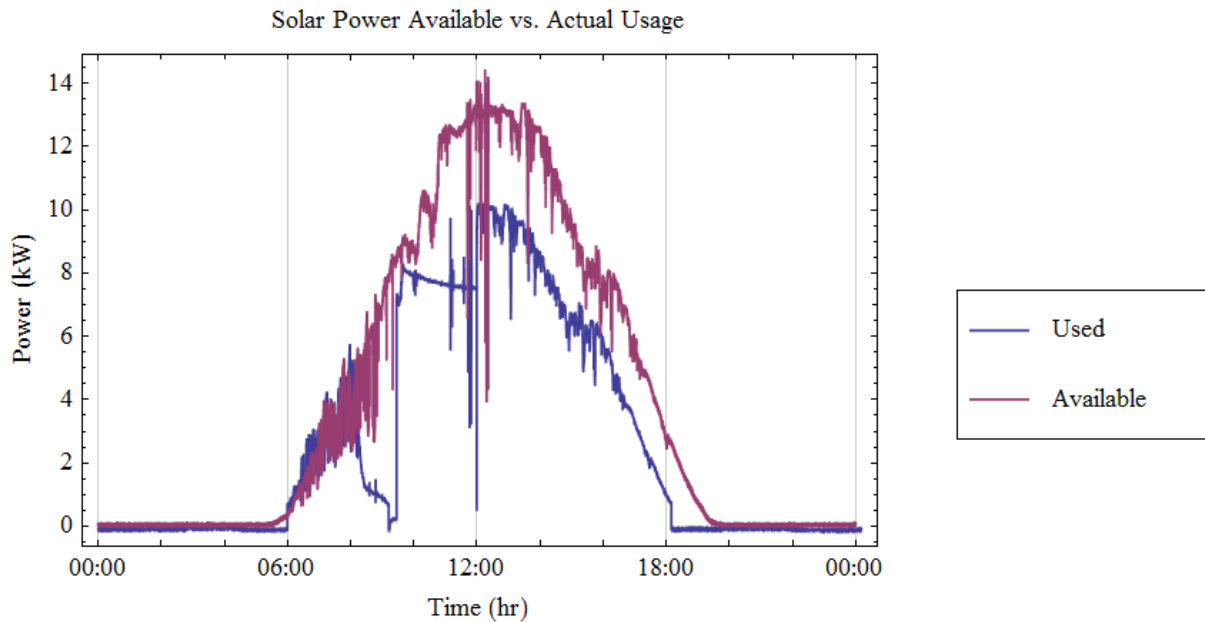


Figure 42. System 3/Load Scenario 2, Available vs. Used Solar Power

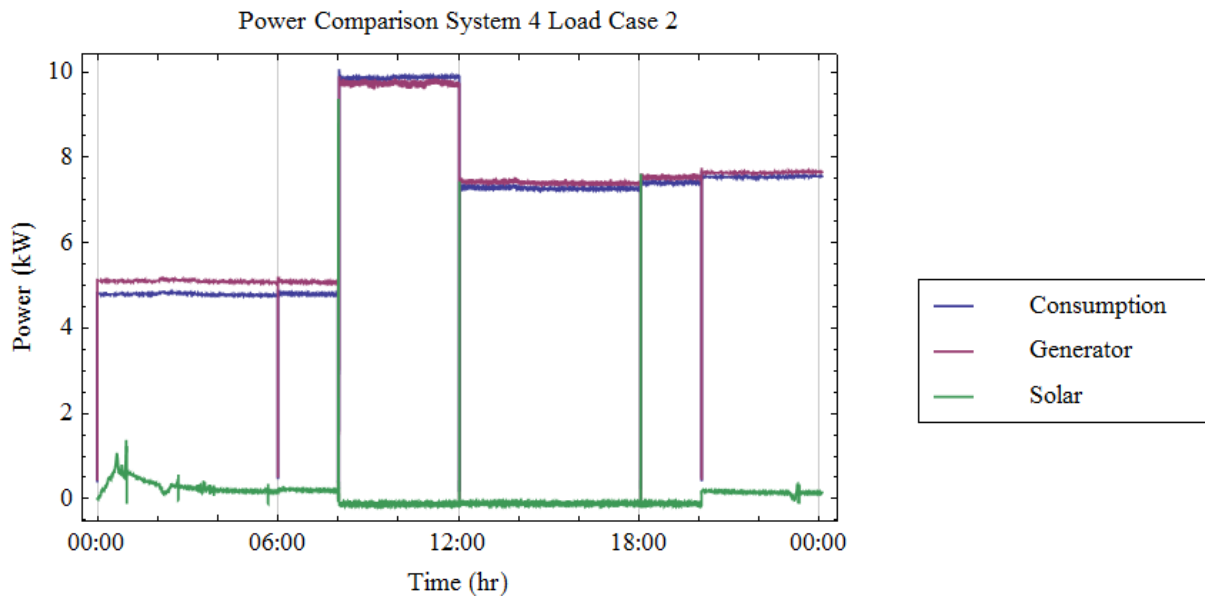


Figure 43. System 4/Load Scenario 2

In Figure 44, the results for System 4, Load Scenario 2 are compared to the available solar power as opposed to the actually consumed solar power. Observation of this graph shows that for a significant percentage of the daylight portion of the test, the solar power was sufficient to meet the power needs of the test, but the requirement to keep the generator running to avoid power outages prevents any savings.

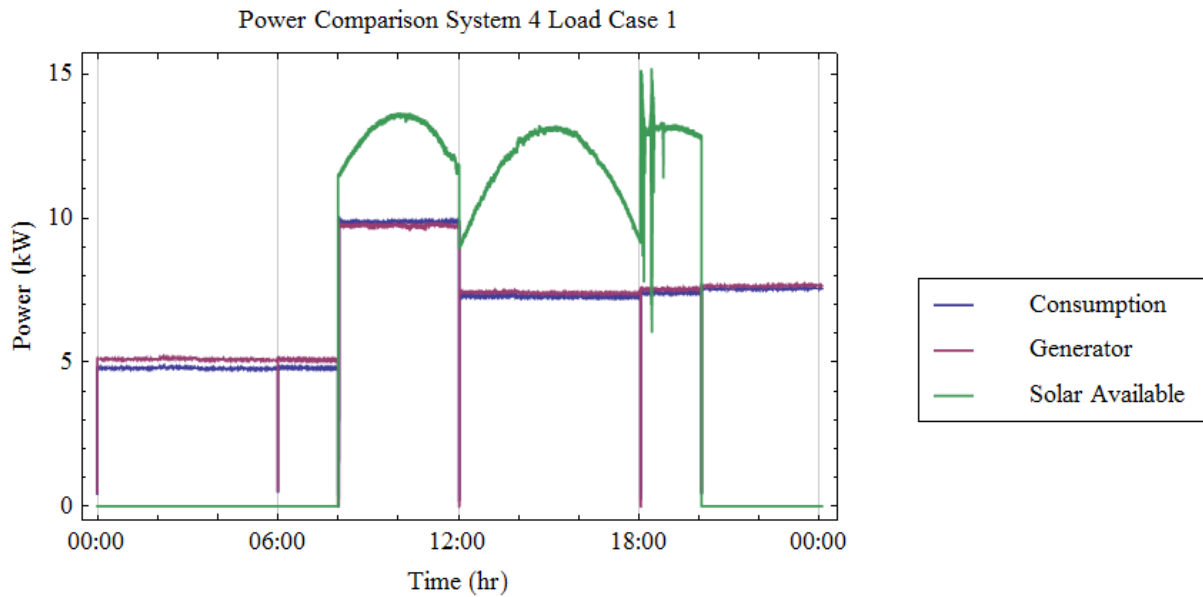


Figure 44. System 4/Load Scenario 2 Available Solar Power

Overall, the behavior of the various system configurations was consistent between the two load cases. As the fuel data shows, the generator does not work as hard to supply energy for the lower levels of Load Scenario 2.

It is also clear from the data that the configuration of the test system does not allow the solar energy to be passed on to the load directly if the generator is running. Investigation is required to determine if a different system configuration would result in a more significant fuel savings with solar power without energy storage.

5. CONCLUSIONS

The data presented reveals several important observations:

- The addition of solar power without a form of energy storage does not result in fuel savings for the power distribution configuration tested. In the case of this test, there was sufficient solar energy available to power a substantial portion of the total load. The fact that the generator needed to be running to avoid power loss prevented this energy from entering the load path, as the generator always had sufficient capacity to meet the load needs. It should be the topic of future analysis to determine if the power circuit could be redesigned in such a way to mitigate this effect.
- The average savings contribution of just adding energy storage is approximately equal to 23 percent, while the addition of solar energy with the storage yields an additional 20 percent, for a combined potential savings of 43 percent averaging the results from the two loads.
- As the power consumption goes down as a percent of maximum power available, the savings potential of either energy storage, or renewable energy along with energy storage, is increased.
- The comparison of fuel consumption of the two load scenarios for System 1 reveals that even substantial reductions in energy demand without a change in energy production results in very little savings. Load Scenario 2 represents an overall 32 percent reduction in energy demand compared to Load Scenario 1, but the data shows only a 12 percent reduction in fuel consumption. A 100 percent reduction in energy demand (no load) results in only a 39 percent reduction in fuel consumption.
- When combined, these results point to a need for systematic control over power production for deployed military forces. Future programs should focus on developing deployable energy storage methodologies and automatic methods for matching energy production to demand levels. These projects will yield far more savings potential than solely adding renewable energy into the deployed setting, and it also shows that simple conservation efforts are also unlikely to show significant savings.
- The authors note that several military "microgrid" programs exist to work on the control of spot generation for the other branches of service. To our knowledge, none of these programs will work within the constraints of the Air Force BEAR Base electrical grid and existing BEAR assets.
- Our test has shown that investing in power production and control methods, along with deployable energy storage and alternative energy has the potential to save up to 43 percent of the fuel used to provide electricity at a deployed base using the BEAR Base power production and distribution systems. For a typical 1100 man deployment, at \$15/gal of fuel and assuming a typical 100 percent over production rate, this would result in a direct savings of 1.7 million gallons of fuel valued at \$25 M/year (assuming currently operating at 100 percent surplus), or 155 million gallons of fuel at \$2.3 B/year for an example 100,000 troop deployment.
- It is believed that the design of an optimized, automated system would likely achieve fuel savings in excess of those reported here.



6. REFERENCES


- Balda, Juan Carlos, and Alejandro R. Oliva. "A PV Dispersed Generator: A Power Quality Analysis Within the IEEE 519." *IEEE Transactions On Power Delivery* 18, 2003: 525-530.
- Braun, Martin. "Conversion and Delivery of Electrical Energy in the 21st Century: Reactive Power Supply by Distributed Generators." *Proc. of Power and Energy Society General Meeting*, 2008: 1-8.
- Braun, Martin, and Thomas Degner. "Development, Verification and Application of a Battery Inverter Model for the Network Analysis Tool PowerFactory." *International Journal of Distributed Energy Resources* 1, 2005: 321-333.
- Casadei, D., G. Grandi, G. Serra, and C. Rossi. "Power quality improvement and uninterruptible power supply using a power conditioning system with energy storage capability." *Power Tech*, 2005, 1 ed.
- Conway, General James, Commandant of the Marine Corps. Verbal Comments, USMC Power and Energy Symposium. February 2010.
- Degner, Thomas, and Martin Braun. "DEVELOPMENT, VERIFICATION AND APPLICATION OF A BATTERY INVERTER MODEL FOR THE NETWORK ANALYSIS TOOL POWERFACTORY." *International Journal of Distributed Energy Resources* 1 (2005). "Development, Verification and Application of a Battery Inverter Model for the Network Analysis Tool Powerfactory." *International Journal of Distributed Energy Resources*, 2005.
- Deloitte. *Energy Security: America's Best Defense*. 2009.
- Engler, ., Degner, T., Braun, M. "Analysis of Inverter-Controlled Island Grids Transient Simulations with ATP-EMTP and PowerFactory." *IEEEExplore*, 2006.
- Jayawarna, N., N. Jenkins, M. Barnes, Et al.. "Safety analysis of a microgrid." *Proc. of International Conference on Future Power Systems.*, 2005.
- Kakigano, Hiraki. "A DC Micro-Grid for Superhigh-Quality Electric Power Distribution." *Electrical Engineering in Japan*, no. 164 (2008): 1207-1214.
- Kariniotakis, G. N., N. L. Sultanis, A. I. Tsouchnikas, S. A. Papathanasiou, and N. D. Hatzargyriou. "Dynamic Modeling of MicroGrids." *Proc. of International Conference on Future Power Systems*, Nov 2005.
- Leung, Eddie. "Surge Protection for Power Grids." *IEEE Spectrum*, July 1997: 26-30.
- Marwali, M. N., Jung Jin-Woo, and A. Keyhani. "Control of distributed generation systems - Part II: Load sharing control." *IEEE Transactions on Power Electronics*, 2004.
- Meliopoulos, A. P. S. "Challenges in simulation and design of μ Grids." *Proc. of IEEE Power Engineering Society*. 27-31 ed. Vol. 1 (2002): 309-314.
- Meliopoulos, A. "Challenges in simulation and design of μ Grids." *Power Engineering Society Winter Meeting*, 2002: 1309-1314.


- Michigami, T., and T. Ishii. "Construction of Fluctuation load model and Dynamic Simulation with LFC control of DC Power System and Frequency Converter Interconnection ." Proc. of Transmission and Distribution Conference, Asia Pacific. Vol. 1., 2002: 382-387.
- O'Gorman, R. "Voltage control for distribution systems."Proc. of International Conference on Future Power Systems, 2005.
- Oliva, A. R. "A PV dispersed generator: a power quality analysis within the IEEE 519." IEEE Transactions on Power Delivery, no. 18 (2003 2003): 525-530.
- Oyarzabal, J, J Jimeno, A Engler, and C Hard. "Agent Based Micro Grid Management System." International Conference on Future Power Systems, IEEE, 18 Nov. 2005.
- Shaffer, Alan R., Principial Deputy Director Defense Research and Engineering. Testimony before the Subcommittee on Readiness of the House Armed Services Committee. March 2009.
- Sharaf, A. M. "A novel hybrid active filter compensator for stabilization of wind-utility grid interface scheme." European Transactions on Electrical Power (Wiley InterScience), 2008.
- Shinji, Takao. "Reduction of Power Fluctuation by Distributed Generation in Micro Grid." Electrical Engineering in Japan 163 (2008): 14-20.
- Takeru, Tawara, Tadahito Aoki, and Yuji Kawagoe. "An Efficient Interactive Inverter for Photovoltaic System." IEEE Proceedings, 1999: 1052-1057.
- U.S. Air Force. Air Force Energy Plan 2010. 2010.


Appendix A: Equipment Specifications


Component Panel Board Equipment and Specifications


Equipment	Specifications		
 Xantrex XW Hybrid Inverter/Charger Model-P/N: WX6048-120/240-60 Qty: 3		<u>120/240</u>	<u>120</u>
	Charge Mode		
	AC Input Voltage Nominal	120/240 V	120 V
	AC Input Current Maximum	60 A	60 A
	AC Input Power Factor	> 0.98	> 0.98
	AC Input Frequency Range	44-68 Hz	44-68 Hz
	DC Output Voltage Range	44-64 V	44-64 V
	DC Output Voltage Nominal	50.4 V	50.4 V
	DC Output Current Maximum	100 A	100 A
	Invert Mode		
	AC Output Voltage Nominal	120/240 V	120 V
	AC Output Frequency Nominal	60 Hz	60 Hz
	AC Output Power Factor	> 0	> 0
	AC Output Current Maximum	50 A	50 A
	AC Output Power Maximum	6000 VA	6000 VA
	AC Output Power Surge (15 sec)	12.0 kVA	12.0 kVA
	DC Input Voltage Range	44-64 V	44-64 V
	DC Input Current Maximum	100 A	100 A
	Utility Mode		
	AC Output Voltage Nominal	240 V	120 V
AC Output Voltage Range	211-264 V	105.5-132 V	
AC output Frequency Nominal	60 Hz	60 Hz	
AC Output Power Factor	> 0.98	> 0.98	
AC Output Current Maximum	30 A	30 A	
AC Power Maximum	6000 W	6000 W	
DC Input Voltage Range	47-58V	47-58 V	
DC Input Current Maximum	100 A	100 A	
 Xantrex Solar Charge Controller Model-P/N: XW MPPT60-150 Qty: 5	Max PV Voltage (Operating)	140 VDC	
	Max PV Open Circuit Voltage	150 VDC	
	Max PV Short Circuit Current	60 A	
	Max Battery Charge Current	60 A	
	Max Battery Charge Voltage	72 VDC	
	Nominal Battery Voltages	12,24,36,48,60 VDC	
	Range of Operating PV Voltage	12-140 VDC	
	Max Output Fault Current	60 A	
	Auxillary Output Terminal	13 VDC, 0.2A	
	Minimum Interrupt Rating	4000 ADC	


 <p>Xantrex Control Panel Model-P/N: XW-SCP Qty: 1</p>	<p>Graphical 128x64 pixel LCD display Large, Tactile Keys Meets UL458 regulatory standards Control/Display of Multiple Network Devices Xanbus Enabled</p>	
---	---	--


 <p>Xantrex Automatic Gen Start Model-P/N: 84-2064-00 Qty: 1</p>	<p>Input Supply Voltage Thermostat Battery Sense Generator AC Input DC Voltage DC Current Operating Temperature Range</p>	<p>12 VDC nominal 12 VDC 12 VDC 120 VAC ±5% at 60 Hz 10- 15.5 VDC 200 mA 0°C – 70°C</p>
---	---	---

 <p>Xantrex Communication Gateway Model-P/N: 975-0330-01-01 Qty: 1</p>	<p>Nominal Input Network Voltage Minimum Operating Network Voltage Maximum Operating Network Voltage Maximum Operating Current Communication Physical Layer Communication Protocol Maximum Xanbus Cable Length Maximum Ethernet Cable Length Connectors Ethernet Wireless Radiated Power</p>	<p>15 VDC 9 VDC 16 VDC 300 mA 2, CAN Xanbus 40 m 60 m 3 RJ-45, 8 pins (2 Xanbus, 1 Ethernet) IEEE Std 802.3 802.11.4b/g 100 mW e.i.r.p max</p>
---	--	--


 <p>Deka/MK Unigy II Energy Storage System Model-P/N: AVR 125-33 Qty: 2 (Series Configuration)</p>	<p>Number Cells per Module Number Plates per Cell Number of Modules Module Voltage Amp Hour C/8 @ 1.75 VPC Volts per Cell Float Voltage per Cell</p>	<p>2 33 12 4 VDC 2000 AH 1.75 VDC 2.25 VDC</p>
---	--	--

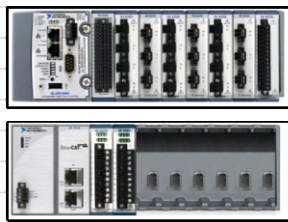
 <p>Eagle Power Solutions AC Load Bank Model-P/N: LB-60-30 Qty: 1</p>	Variable Load Range (on 3-Phase)	1 - 30 kW	
	Variable Load Range (on Single Phase)	1-20 kW	
	Meters	0-150 V Voltmeter 0-100 A Ammeter 55-65 Hz Freq. Meter	
	120/240 Single Phase or 120/208 3-Phase		
	Thermal Protection		


 <p>Xantrex XW Power Distribution Panel Model-P/N: 865-1015 Qty: 2</p>	Accommodates AC/DC breakers and wiring for three XW Hybrid Inverter/Chargers and four XW Solar Charge Controllers		
	Multiple Knockouts on sides, top, bottom, and back of unit Includes Mounting back plate and XW Conduit Box		


 <p>CR Magnetics Transducers Model-P/N: Selected Qty: CR5320-200 x 1 CR5320-50 x 1 CR5210-400 x 1 CR5210S-20 x 1 CR5210-150 x 3 CR2RL-1250 x 3 CR5210-20 x 1</p>			
	Voltage	Input	Output
	CR5320-200	0 - 200 VDC	4 - 20 mA
	CR5320-50	0 - 50 VDC	4 - 20 mA
	Current		
	CR5210-400	0 - 400 A	- 5 to 5 VDC
	CR5210S-20	0 - 20 A	- 5 to 5 VDC
	CR5210-150	0 - 150 A	- 5 to 5 VDC
	CR2RL-1250, (125:5 ratio)	0 - 760 A	0 - 5 ARMS
	CR5210-20	0 - 20 A	0 - 5 VDC


Data Acquisition Enclosure Equipment and Specifications


Equipment	Specifications	
		
NEMA Outdoor Enclosure Model-P/N: OD-50DDXC Qty: 1	Doors 2, secured by three point locking system Sealed with 0.875" AI filled gaskets	
	Material Enclosure Material RF Properties	0.125" Alumiflex Non-Ferrous
	Rails Holes tapped 10-32 threads Alodine coated	
	Material Spacing	0.12" Alumiflex 19" rack mount
	Number of Rack Units/Rail Set	26
	Total Number RU's	52
	Ratings NEMA 3R (Vented) Nema 4 (closed loop-a/c) Nema 4X	
	Dimensions Exterior Main Body	50.23" x 25.5" x 42"


		
National Instruments cRIO Hardware	Controller NI-cRIO-9024	
	Chassis NI-cRIO-9114 NI-cRIO-9144 EtherCAT Slave Chassis	8 slot 8 slot
Model-P/N: Selected	Voltage NI-cRIO-9205 NI-cRIO-9225	AI ± 10V AI 300 VRMS
Qty: NI-cRIO-9024 x 1		
NI-cRIO-9114 x 1 NI-cRIO-9144 x 1	Current NI-cRIO-9227 NI-cRIO-9203	AI 5 ARMS AI ± 20 mA
NI-cRIO-9205 x 1 NI-cRIO-9225 x 3 NI-cRIO-9227 x 3	Digital NI-cRIO-9421 NI-cRIO-9474	DI 24V Sink DO 24V Source
NI-cRIO-9203 x 1 NI-cRIO-9421 x 1 NI-cRIO-9474 x 1		


	Power	
	Input Voltage	24 VDC
National Instruments Unmanaged Ethernet Switch Model-P/N: NI-UES-3880 Qty: 1	Input Current	0.25 A @ 24VDC
	Overload Current Protection	1.1 A
	Reverse Polarity Protection	Present
	Interface	
	Number of 10/100BASE-T(X) RJ45 ports	8
	Standards	IEEE 802.3/u/x
	LED Indicator	PWR1, PWR2, Fault
	DIP Switch	10/100M, 100M Port Break Alarm Mask

	15" XGA/TFT color LCD Touch Screen	
	Processor	2.0 GHz Pentium 4
National Instruments Touchscreen Panel PC Model-P/N: NI-PPC-2015 Qty: 1	RAM	512 MB
	Hard Drive	40 GB
	Additional Drives	CD-ROM, Floppy
	Communication	
	Number of Ethernet ports	1
	Number of USB ports (USB 2.0)	5
	Number of RS232 ports	2
	Number of PCMCIA ports (Type II)	2
	Number of IEEE 1394 ports	2
	Number of PS/2 ports	2




	Voltage Output	
	24 VDC @ 10A	
Sola Power Supply Model-P/N: SDN-10-24-100P Qty: 1	Configuration	Enclosed
	Current, Rating	5/2 A
	Frequency	47 - 63 Hz
	Mounting	DIN Rail
	Number of Outputs	1
	Power Output	240 W
	Primary Type	AC-DC
	Voltage Input	85 - 264/210 to 375 VAC/VDC
	Voltage Rating	115/230 VAC

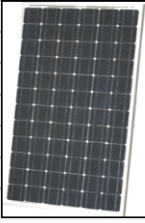
	Mounting Style	
	RL	
CR Magnetics Current Transformer Model-P/N: CR1ARL-760 Qty: 6	Current Rating	75:5
	Frequency	50 - 400 Hz
	Insulation	0.6 kV, BIL 10 kV Full Wave


 <p>Fuji IEC Contactor Model-P/N: SC-E5-24V Qty: 4</p>	Standard Rating	IEC
	Device Technology	Electro-Mechanical
	AC Motor Phase	3
	Starter Ratings	
	Thermal Current	150 A
	Motor Voltage	24 VDC
	Three Phase Power	75.00 HP
	Number of Poles	4 (2 N.O, 2 N.C)
	Coil Voltage	24 VAC/VDC

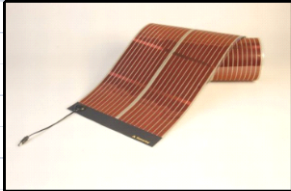
 <p>CyberPower UPS Model-P/N: PR1500LCDRT2U Qty: 1</p>	Line-Interactive Topology	
	2U Rack Mount	
	Multi-Function Rotatable LCD Display	
	SNMP/HTTP remote management	
	Input	
	Voltage	80- 150 VAC
	Frequency	50/60 Hz
	Output	
	Outlets - Battery & Surge Protection	8
	Outlets - Critical Load	4
	VA	1500
	Watts	1000
	Connections/Communications	
	Number of HID USB ports	1
	Number of DB9 Serial ports	2
	Number of EPO ports	1
	Number of RJ11/RJ45 ports	3 (1 RJ11, 2 RJ45)
	Number of RG-6 connections	2
Battery		
Runtime @ Half Load	18 min	
Runtime @ Full Load	6 min	
Recharge Time	8 hours	


RETC Outdoor Equipment and Specifications

Equipment	Specifications	
 Generator Set Model-P/N: MEP-805A Qty: 1	Generator Set	Volts 120/208/240/416 VAC Frequency 50/60 Hz Speed 1800 RPM Phase 3 Rated Power 30 kW
	Engine	Type 4 Cycle Cylinders 4 Displacement 3.9 L Horsepower 92 @ 1800 RPM Compression 17.8 : 1
	Fuel	Capacity 23 Gal Fuel Consumption 2.60 GPH Fuel Requirement Diesel/JP-8
	Aural Signature	Audio Rating 70 dBA @ 7 m
 Secondary Distribution Center (SDC) Model-P/N: SDC-10 Qty: 1	Input Voltage 2400/4160 VAC, 3-Phase Frequency 60 Hz Output Voltage 120/208 VAC, 3-Phase Total Power Rating 150 kVA Output Current 416 A Number of 60 A output Connections 16 Number of MEP Inputs Connections 1 Number of Loadbreak Elbow Receptacles 9	
 Primary Distribution Panel (PDP) Model-P/N: PEU-156/E Qty: 1	Power Rating 25 kW Input Power 120/208 - 3 Phase, 60 A Number of Input Connections 1 Output Power 120/208 - 3 Phase, 60 A 120 VAC - 1 Phase, 20 A 120 VAC - 1 Phase, 15 A Number of Output Connections 4 x 120/208 - 3 Phase, 60 A 2 x 120 VAC - 1 Phase, 20 A 1 x 120 VAC - 1 Phase, 15 A	

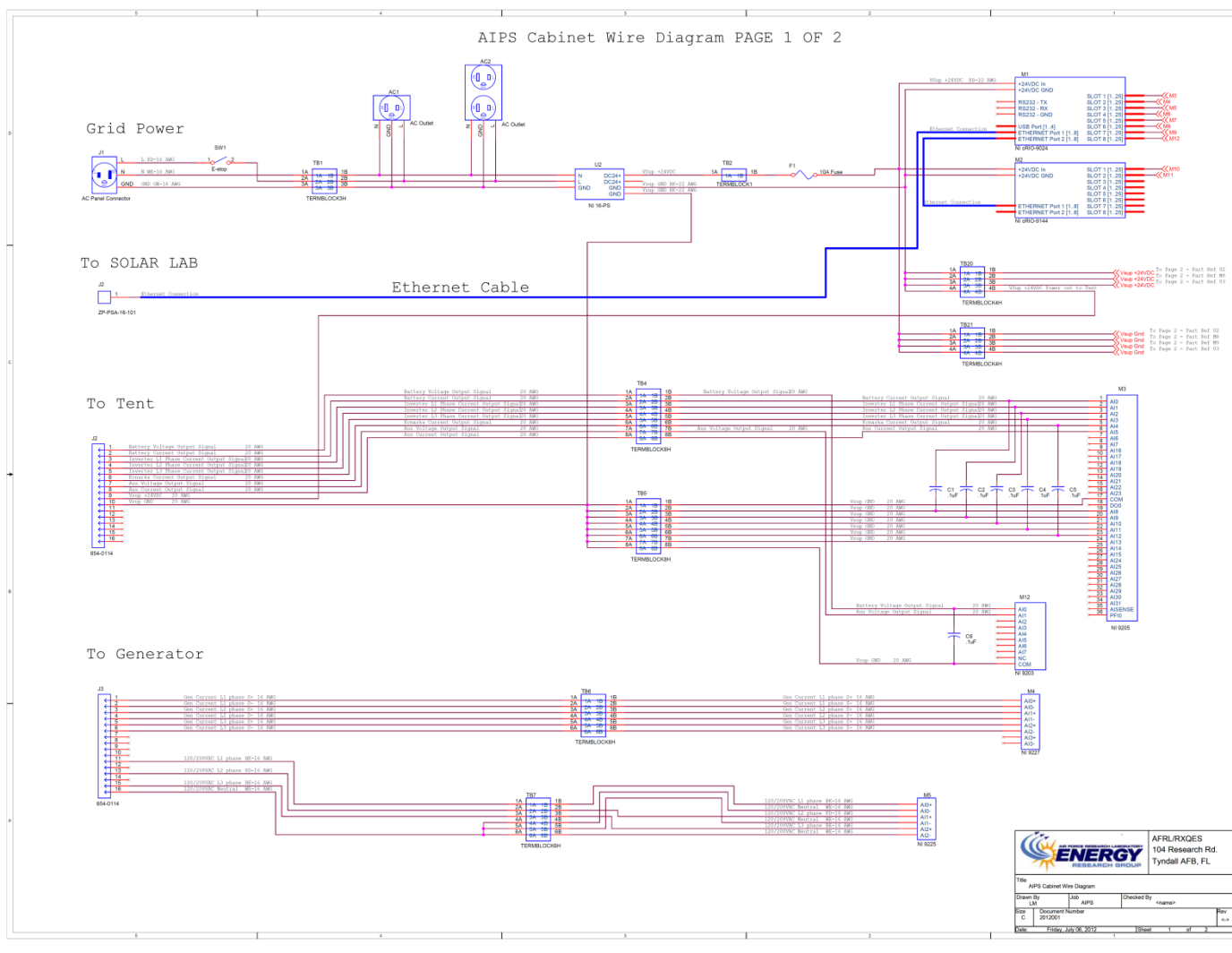
 <p>SolarWorld Photovoltaic Panel Model-P/N: SW 175 Qty: 70</p>	Type	Monocrystalline
	Rated Maximum Power	175 W
	Open Circuit Voltage	44.4 V
	Rated Voltage	35.8 V
	Short Circuit Current	5.3 A
	Rated Current	4.9 A

 <p>Utilis Shelter System Model-P/N: TM60 Qty: 1</p>	Length	34 ft
	Width	19 ft
	Height	9 ft
	Weight	937 lb

 <p>Konarka Thin Film Solar Panel Model-P/N: Power Series 40 Qty: 60</p>	Voltage at Maximum Power Point	15.8 V
	Open Circuit Voltage	22.6 V
	Current at Maximum Power Point	1.6 A
	Short Circuit Current	1.9 A
	Rated Power	24.7 W

 <p>Apogee Silicon-Cell Pyronometer Model-P/N: SP-110-L-46 Qty: 8</p>	Absolute Accuracy	± 1%
	Sensitivity	Custom Calibrated to 5.00 W/m ² per mV
	Uniformity	± 3%
	Cosine Response: 45° zenith angle	± 1%
	Cosine Response: 75° zenith angle	± 5%
	Linear Output Range	0-350 mV
	Input Power	None, Self Powered

Appendix B: AIPS Electrical Schematic Diagrams



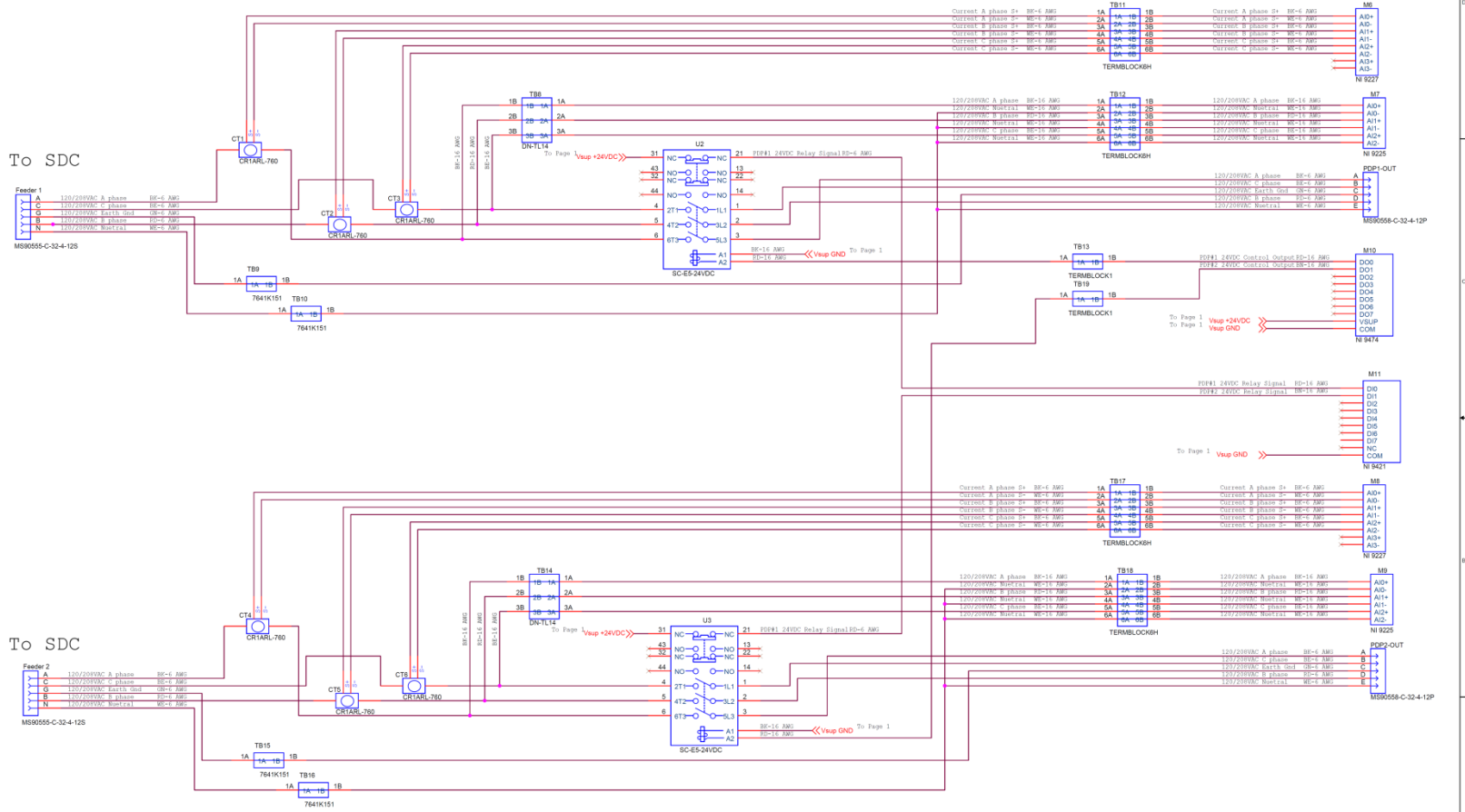
AIPS Cabinet Wire Diagram PAGE 2 OF 2

To SDC

Feeder 1
MS9055-C-32-4-125

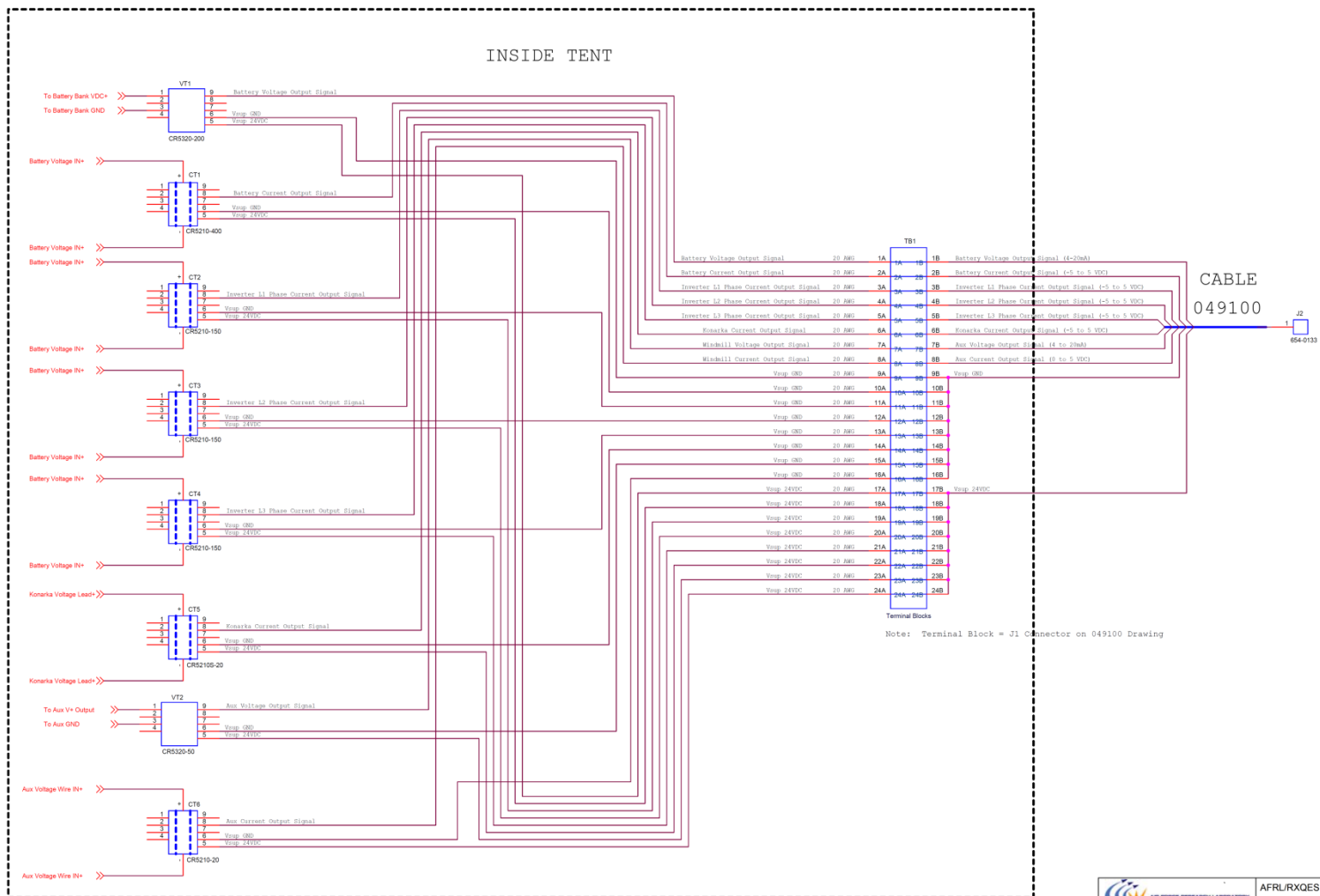
To SDC

Feeder 2
MS9055-C-32-4-125



		AFRL/RXQES	
		104 Research Rd. Tyndall AFB, FL	
Title AIPS Cabinet Wire Diagram			
Drawn By LM	Job AIPS	Checked By <name>	Rev <->
Size C	Document Number 201001		
Date Friday, July 26, 2012	Sheet 2	of 3	

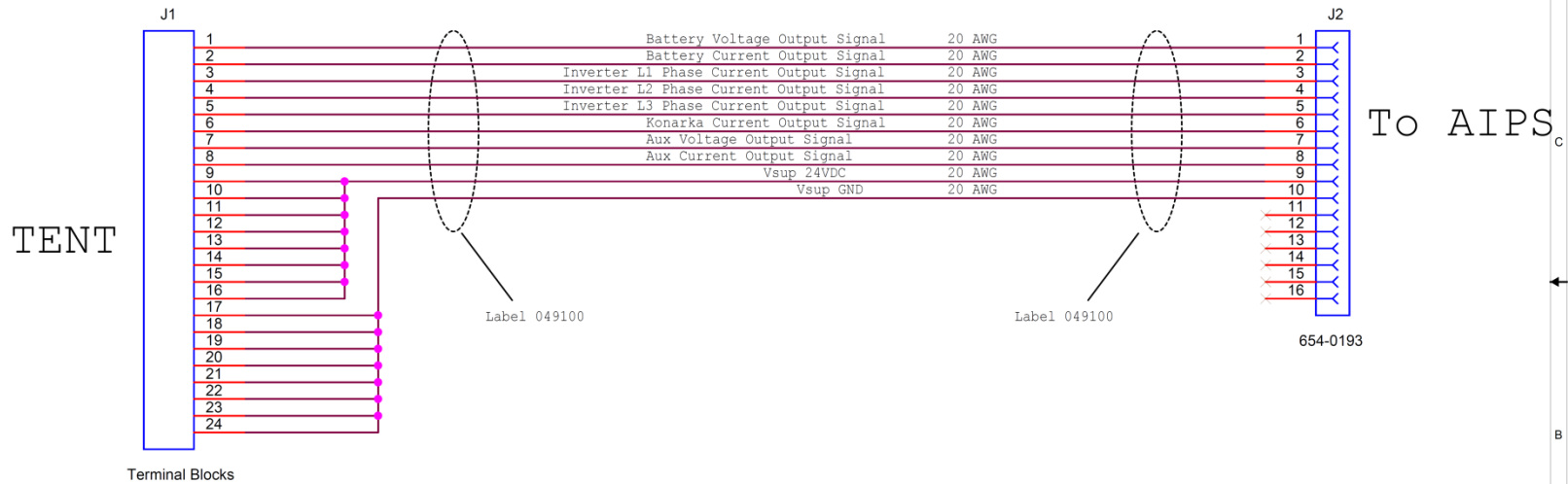
AIPS Tent Sensors Wire Diagram



		AFRL/RXQES 104 Research Rd. Tyndall AFB, FL	
Title: AIPS Tent Sensors Wire Diagram			
Drawn By: GW	Job: <job name>	Checked By: <name>	
Size: C	Document Number: 2012002	Rev: <->	
Date: Friday, July 06, 2012		Sheet: 1 of 1	

AIPS Tent Sensor Cable

Length Approx. 25' (Tent to AIPS Cabinet)

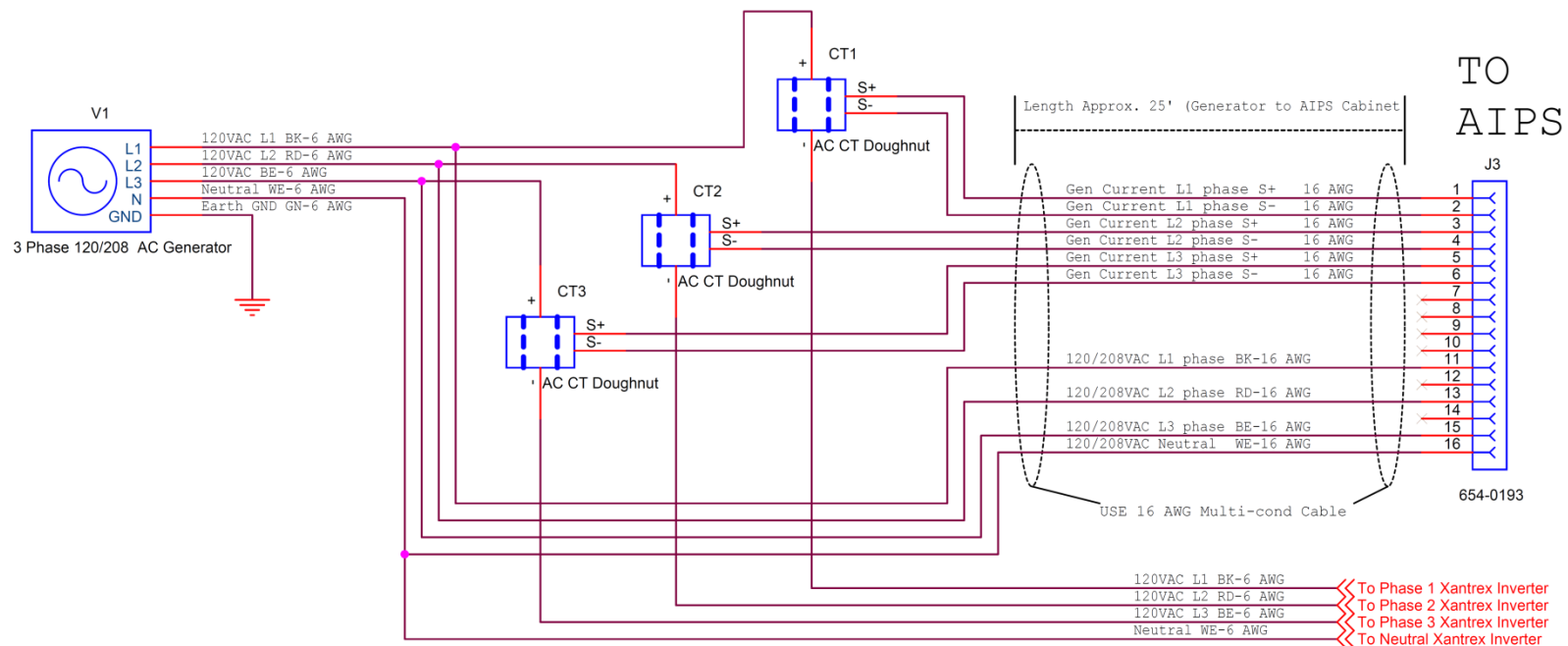



Note: Use 8 Triple Level Terminal Blocks

- Use 20 AWG (8 twisted pair) shielded cable
- Make Bottom Level Gnd Bus
- Make Center Level Voltage bus
- Make Top Level Signal Inputs from Voltage and Current Transducers

		AFRL/RXQES 104 Research Rd. Tyndall AFB, FL	
Title AIPS Tent Sensor Cable			
Drawn By LM		Job <job name>	Checked By <name>
Size A	Document Number 049100		Rev <->
Date: Friday, July 06, 2012		Sheet 1 of 1	

30kW Generator Sensor Cable



		AFRL/RXQES 104 Research Rd. Tyndall AFB, FL	
		Title 30kW Generator Sensor Cable	
Drawn By LM	Job AIPS	Checked By <name>	
Size A	Document Number 2012003		Rev <->
Date: Friday, July 06, 2012		Sheet 1 of 1	2

LIST OF SYMBOLS, ABBREVIATIONS, AND ACRONYMS

A	ampere
AC	alternating current
AFRL	Air Force Research Laboratory
AGM	absorbed glass mat
AIPS	Advanced Integrated Power Systems
B	billion
BEAR	Basic Expeditionary Airfield Resource
CERDEC	Communications-Electronics Research, Development, and Engineering Center
DC	direct current
DOD	depth of discharge
ECU	environmental control unit
gal	gallon
HPFC	hybrid power filter compensator
hr	hour(s)
HTS	high temperature superconductors
HTTP	hypertext transfer protocol
HVAC	heating, ventilation and air conditioning
Hz	hertz
GB	gigabyte
IEEE	Institute of Electrical and Electronics Engineers
I/O	input/output
JADE	Java development framework
kg	kilogram
kW	kilowatt
LabVIEW	Laboratory Virtual Instrumentation Engineering Workbench
Li	lithium
M	million
m	meter(s)
MEP	mobile electric power
MTP	messenger transport protocol
MW	megawatt
NEMA	National Electrical Manufacturers Association
NI	National Instruments
Na	sodium
PC	personal computer
PDC	primary distribution center
PDP	primary distribution panel
PV	photovoltaic
RAM	random access memory
RETC	Renewable Energy Tent City
S	silicon
SDC	secondary distribution center
UPS	uninterrupted power supply
USMC	United States Marine Corps

V	volt
VI	Virtual Instrument
VSC	voltage source converter
W	Watt